



# The effects of trade-off shape and dimensionality on eco-evolutionary dynamics in resource competition

Jonas Wickman<sup>a,b,\*</sup>, Christopher A. Klausmeier<sup>ID a,b,c,d</sup>

<sup>a</sup> W. K. Kellogg Biological Station, Michigan State University, Hickory Corners, MI, USA

<sup>b</sup> Program in Ecology, Evolution, and Behavior, Michigan State University, East Lansing, MI, USA

<sup>c</sup> Department of Integrative Biology, Michigan State University, East Lansing, MI, USA

<sup>d</sup> Department of Plant Biology, Michigan State University, East Lansing, MI, USA

## ARTICLE INFO

### Keywords:

Adaptive dynamics

Community assembly

Limiting factors

## ABSTRACT

Organisms invariably experience trade-offs in their capacities for interacting with their environments. In resource competition, this often means that an organism's ability to acquire one resource can only come at the cost of less ability with others. If the traits governing resource acquisition are under selection and heritable, this will induce eco-evolutionary dynamics along the trade-off. For Lotka–Volterra models derived from MacArthur resource competition models and for explicit resource models with two resources, the shape and dimensionality of trade-offs has seen substantial study. However, how the joint effects of trade-off shapes and the number of resources under competition affect eco-evolutionary outcomes has seen relatively little. For example, is diversification through evolutionary branching more or less likely when the number of resources increases? Here, we will present techniques complementary to existing ones for recasting trade-offs in an implicit form. Combining adaptive dynamics and resource-competition theory, we derive expressions for directional and stabilizing/disruptive selection. We apply our techniques to two models of resource competition and investigate how the number of resources and trade-off shapes affect the stability characteristics of the generalist strategy, and how diverse a community of consumers can be assembled through successive evolutionary branching. We find that even for these simple and highly symmetric models, outcomes are surprisingly complex and idiosyncratic. Taken together, our results deepen our understanding of the eco-evolutionary dynamics of resource competition for multiple resources.

## 1. Introduction

The fitness of an organism depends on its interactions with its environment, such as taking up nutrients or hunting prey, defending against predation, or neutralizing toxic compounds. In an ideal world for this organism, evolution would gradually improve all these capacities to maximize fitness over time. However, due to constraints of physics, physiology, or genetics this is never possible and trade-offs between the organism's capacities to interact with its environment will eventually emerge. In resource competition, trade-offs may manifest in, for example, the beetle morphology that allows easier capture of smaller or larger snails (Konuma et al., 2013) or in phytoplankton trading nitrogen-uptake ability for phosphorous-uptake ability (Edwards et al., 2011). The eco-evolutionary consequences of trade-offs in competition for two resources have a long history of theoretical study (Levins, 1962; MacArthur and Levins, 1967; Lawlor and Smith, 1976; Rueffler et al., 2006; Koffel et al., 2016; Wickman et al., 2019; Vasconcelos and Rueffler, 2020), in particular with regards to whether a trade-off engenders

two coexisting resource specialists or one single generalist, and whether these specialists can evolve from a single generalist through evolutionary branching, where an initially monomorphic population evolving according to directional selection eventually ends up at a fitness minimum and experiences disruptive selection leading to two new ecotypes (Geritz et al., 1998; Dieckmann and Doebeli, 1999).

A firm understanding of eco-evolutionary dynamics in competition for pairs of resources serves as an important foundation for answering these questions; yet, organisms frequently compete for more than two resources. For example, in addition to nitrogen and phosphorous, phytoplankton may require several other essential elements such as silicon or iron, and often compete for more than one source of carbon (Sandrini et al., 2013), soil microbes are affected by the diversity of carbon compounds available (Kinkel et al., 2011), and heterotrophs frequently graze or predate on several plants or animals (Middleton et al., 2021; DeSantis et al., 2022). While all factors required by organisms need not be actively competed for (for example, oxygen for terrestrial organisms), multi-resource competition is still likely a

\* Corresponding author.

E-mail address: [jonas.wickman@gmail.com](mailto:jonas.wickman@gmail.com) (J. Wickman).

common occurrence. In implicit Lotka–Volterra competition models in the style of MacArthur (1970), multidimensional resource competition has seen substantial study. In these models, resource diversity is over an ordered continuum of resource properties (such as small-to-large seed sizes), and evolutionary diversification tends to become more likely the more high-dimensional this resource space is (Doebeli and Ispolatov, 2010; Débarre et al., 2014; Svardal et al., 2014), although it has been remarked that this only applies when the Lotka–Volterra model is based on substitutable resources (Ashby et al., 2017). However, theory and models investigating the role of trade-offs in the eco-evolutionary dynamics of competition for explicit discrete resources, such as different chemical compounds for autotrophs or distinct prey species for heterotrophs, has scarcely seen any study for more than two resources (but see Caetano et al., 2021). In particular, it is not well understood how well-known results regarding trade-off shapes for two resources scale up to multiple resources, and outcomes only possible with more than two resources, such as multiple successive evolutionary branching events, are underexplored. For example, for two substitutable or complimentary resources (*sensu* Tilman, 1980), a common pattern is that as the trade-off shape changes from generalist-favoring to increasingly specialist-favoring, the eco-evolutionary stability characteristics of the generalist strategy go from being attractive and evolutionarily stable, to an evolutionary branching point where monomorphic populations are attracted towards generalism, but where the generalist strategy is not evolutionarily stable and splits into two consumers that subsequently evolve opposite specializations, and finally to an evolutionary repellor, where monomorphic populations evolve towards specialism anywhere on the trade-off curve (Rueffler et al., 2006; Wickman et al., 2019; Gonzalez et al., 2022). For more than two resources, we can ask not only whether this pattern holds for the generalist strategy for an increasing number of resources, but also whether subsequent evolutionary branchings can occur and how diverse a community of consumers can be attained through successive evolutionary branching events.

One possible reason that multi-resource models have seen little study, apart from multivariate adaptive dynamics being more complicated overall (Leimar, 2001, 2009; Geritz et al., 2016), is that the typical way to implement trade-offs in two-resource models has been through parameterization, where a consumer's facility with either resource are set to be functions of a single parametric trait. While this approach in principle could be used also for higher dimensionalities—using two parametric traits for three resources, three parametric traits for four resources, and so on—in practice, taking a given parameterization between two traits and generalizing it to higher dimensionalities is difficult. The stability characteristics of evolutionarily singular points do not depend on any specific parameterization, only the shape of the trade-off (de Mazancourt and Dieckmann, 2004; Bowers et al., 2005; Kisdi, 2015), which means that mathematical descriptions other than parameterization of trade-offs could be used to constrain traits. Using a Lagrange-multiplier method, Ito and Sasaki (2016) showed how trade-off constraints described by an implicit function could be incorporated into expressions describing the stability characteristics of evolutionarily singular points.

In this paper, we develop an alternative derivation to Ito and Sasaki (2016) using projection for how implicitly described trade-offs can be incorporated into adaptive dynamics and combine it with a model of competition mediated by limiting factors, such as resources or predators. We derive expressions for evaluating directional and stabilizing/disruptive selection, as well as for convergence stability where all expressions are based on the model ingredients of the species' traits and densities, and the densities of limiting factors. To see how increasing the number of resources changes how trade-off shapes affect eco-evolutionary outcomes we generalize two previously studied two-resource competition models (Lawlor and Smith, 1976; Rueffler et al., 2006; Schreiber and Tobiason, 2003; Wickman et al., 2019). Recasting the parametric trade-offs in these models to implicit form, we show how they can be easily generalized to an arbitrary number of dimensions. Using the gen-

eral expressions we developed, we derive analytical expressions for how the stability characteristics of the generalist strategy changes across different trade-offs and with the number of resources for our first simpler model, and use a combination of analytical and numerical methods for our second more involved model. We find that whether the number of resources affects the stability of the generalist strategy depends on the details of how trade-offs are generalized to more dimensions. We numerically explore how trade-off shapes and the number of resources affect evolved diversity through successive evolutionary branchings and find that surprisingly complex patterns of diversity emerge given the relative simplicity and high degrees of symmetry in our two example models.

## 2. Methods

In this section we will first review some results from adaptive dynamics (Metz et al., 1992; Dieckmann and Law, 1996; Geritz et al., 1998; Dercole and Rinaldi, 2008), and introduce our model together with its associated notation. We will then introduce how we describe trade-off constraints implicitly and how these can be incorporated into the adaptive dynamics of our model.

### 2.1. Adaptive dynamics without trade-offs

Before we lay out our approach to incorporating trade-offs, we will begin by briefly reviewing the standard results for adaptive dynamics without trait constraints and introduce our study system and notation. Apart from explicitly writing out equations for the limiting factors, our presentation here mostly follows Leimar (2009) and Geritz et al. (2016).

We consider organisms with a trait vector  $\mathbf{x} = (x_1, x_2, \dots, x_d) \in \mathbb{R}^d$ , where each trait component  $x_i$  encodes some property of the organism, such as the ability to take up a specific resource. Write  $N$  for the density of a single resident species of the organism and  $\mathbf{E}' = (E'_1, E'_2, \dots, E'_n)$  for the vector of environmental variables, such as resources, predators, or toxins. We write  $\mathbf{E} = (\mathbf{E}', N)$  for the environment experienced by individuals, which also includes the density of the species itself. We let the instantaneous per capita growth rate of a rare strain with trait vector  $\mathbf{x}$  in the environment  $\mathbf{E}$  be given by  $g(\mathbf{x}, \mathbf{E})$ . For a given resident with trait vector  $\mathbf{x}_{\text{res}}$  the ecological dynamics are thus described by

$$\frac{dN}{dt} = g(\mathbf{x}_{\text{res}}, \mathbf{E})N, \quad (1a)$$

$$\frac{d\mathbf{E}'}{dt} = \mathbf{f}(\mathbf{x}_{\text{res}}, \mathbf{E}), \quad (1b)$$

where  $\mathbf{f} = (f_1, f_2, \dots, f_n)$  are the functions governing the dynamics of the environmental variables. When extended to multiple species, this formulation assumes that any frequency-dependent interactions are mediated by the limiting factors.

As is standard in adaptive dynamics, we will assume a separation of time scales with the ecological variables changing much faster than the traits, and we will restrict ourselves to the case of ecological equilibrium dynamics. We denote the ecological equilibrium by  $\mathbf{E}^*$ , which is implicitly defined through

$$0 = g(\mathbf{x}_{\text{res}}, \mathbf{E}^*), \quad (2a)$$

$$\mathbf{0} = \mathbf{f}(\mathbf{x}_{\text{res}}, \mathbf{E}^*). \quad (2b)$$

Furthermore, we will assume, at least locally around  $\mathbf{E}^*$ , that  $\mathbf{E}^* = \mathbf{E}^*(\mathbf{x}_{\text{res}})$ , which is to say that the equilibrium environment is a function of the resident trait. The central concept to determine trait evolution in adaptive dynamics is the invasion fitness of a rare invader with trait vector  $\mathbf{x}$  in the environment set by a resident with trait vector  $\mathbf{x}_{\text{res}}$ , which we will denote by  $\rho(\mathbf{x}, \mathbf{x}_{\text{res}})$ . The invasion fitness is the long-term exponential growth rate while the invader is still rare, which for our system is given by

$$\rho(\mathbf{x}, \mathbf{x}_{\text{res}}) = g(\mathbf{x}, \mathbf{E}^*(\mathbf{x}_{\text{res}})). \quad (3)$$

In the following, we will need to take multivariate derivatives of the invasion fitness. As we will need to combine these derivatives with various linear-algebra operations, we will introduce some short-hand notation; again following Geritz et al. (2016), but being more explicit about what constitutes a column or row vector. We will write

$$\mathbf{x} = (x_1, x_2, \dots, x_d) = \begin{bmatrix} x_1 \\ x_2 \\ \vdots \\ x_d \end{bmatrix} \quad (4)$$

for a column vector, and  $\mathbf{x}^T = [x_1 \ x_2 \ \dots \ x_d]$  for the row vector with the same entries. When differentiating a scalar function  $g$ , we write  $\partial g / \partial \mathbf{x}$  as the short-hand for the column vector of partial derivatives of  $g$  and  $\partial g / \partial \mathbf{x}^T$  is the row vector with the same entries. When differentiating a vector function  $\mathbf{f}$ ,  $\partial \mathbf{f}(\mathbf{x}) / \partial \mathbf{x}^T$  is the Jacobian matrix of the function so that  $(\partial \mathbf{f} / \partial \mathbf{x}^T)_{ij} = \partial f_i / \partial x_j$ , and  $\partial \mathbf{f}^T / \partial \mathbf{x}$  is its transpose. For mixed second-order derivatives of scalar functions  $\partial^2 g(\mathbf{x}, \mathbf{y}) / \partial \mathbf{x} \partial \mathbf{y}^T$  is a matrix with entries  $(\partial^2 g(\mathbf{x}, \mathbf{y}) / \partial \mathbf{x} \partial \mathbf{y}^T)_{ij} = \partial^2 g / \partial x_i \partial y_j$ , and  $\partial^2 g / \partial \mathbf{x} \partial \mathbf{x}^T$  is the Hessian matrix of  $g$ .

Under assumptions of rare and small mutations (Dieckmann and Law, 1996; Champagnat, 2003) or under assumptions of small standing trait variation (Lande, 1979, 1982), directional selection determining how the trait of a resident  $\mathbf{x}_{\text{res}}$  will evolve over time will be determined by the selection gradient

$$\gamma(\mathbf{x}_{\text{res}}) := \frac{\partial \rho(\mathbf{x}, \mathbf{x}_{\text{res}})}{\partial \mathbf{x}} \Big|_{\mathbf{x}=\mathbf{x}_{\text{res}}} = \begin{bmatrix} \partial \rho / \partial x_1 \\ \partial \rho / \partial x_2 \\ \vdots \\ \partial \rho / \partial x_d \end{bmatrix} \Big|_{\mathbf{x}=\mathbf{x}_{\text{res}}} = \frac{\partial g(\mathbf{x}, \mathbf{E}^*(\mathbf{x}_{\text{res}}))}{\partial \mathbf{x}} \Big|_{\mathbf{x}=\mathbf{x}_{\text{res}}} \quad (5)$$

In particular, if  $\gamma(\mathbf{x}^*) = \mathbf{0}$  then directional trait evolution will cease at  $\mathbf{x}_{\text{res}} = \mathbf{x}^*$ , which is known as an evolutionarily singular point (or evolutionarily singular strategy). The evolutionary behavior around such a point is determined by second-order derivatives of the invasion fitness (Leimar, 2009; Geritz et al., 2016). In particular, for an evolutionarily singular point  $\mathbf{x}^*$  we define the selection Hessian matrix

$$\mathbf{H} := \frac{\partial^2 \rho(\mathbf{x}, \mathbf{x}_{\text{res}})}{\partial \mathbf{x} \partial \mathbf{x}^T} \Big|_{\mathbf{x}=\mathbf{x}_{\text{res}}=\mathbf{x}^*} \quad (6)$$

and the selection Jacobian matrix

$$\mathbf{J} := \frac{\partial \gamma(\mathbf{x}_{\text{res}})}{\partial \mathbf{x}_{\text{res}}^T} \Big|_{\mathbf{x}_{\text{res}}=\mathbf{x}^*} = \frac{\partial^2 \rho(\mathbf{x}, \mathbf{x}_{\text{res}})}{\partial \mathbf{x} \partial \mathbf{x}^T} \Big|_{\mathbf{x}=\mathbf{x}_{\text{res}}=\mathbf{x}^*} + \frac{\partial^2 \rho(\mathbf{x}, \mathbf{x}_{\text{res}})}{\partial \mathbf{x} \partial \mathbf{x}_{\text{res}}^T} \Big|_{\mathbf{x}=\mathbf{x}_{\text{res}}=\mathbf{x}^*} \quad (7)$$

The selection Hessian  $\mathbf{H}$  measures the curvature of the invasion-fitness landscape around  $\mathbf{x}^*$ . For a scalar trait  $x$ , it would simply be the second derivative of the invasion fitness with respect to the invader trait,  $H_{\text{scalar}} = \partial^2 \rho(x, x_{\text{res}}) / \partial x^2|_{x=x_{\text{res}}=x^*}$ . The selection Jacobian  $\mathbf{J}$  measures the local stability of the singular point  $\mathbf{x}^*$  for the resident dynamics, determining whether residents are attracted to or repelled by  $\mathbf{x}^*$ . For a scalar trait, the selection Jacobian could be expressed as  $J_{\text{scalar}} = \partial^2 \rho(x, x_{\text{res}}) / \partial x^2|_{x=x_{\text{res}}=x^*} + \partial^2 \rho(x, x_{\text{res}}) / \partial x \partial x_{\text{res}}|_{x=x_{\text{res}}=x^*}$ .

To determine evolutionary outcomes near the evolutionarily singular point, write  $\lambda_H$  for the dominant eigenvalue of  $\mathbf{H}$ . Then,  $\mathbf{x}^*$  is said to be an evolutionarily stable strategy (ESS) if  $\lambda_H < 0$ , which means that  $\mathbf{x}^*$  is locally uninvasive by any nearby strategy. Conversely, if  $\lambda_H > 0$  there exists some nearby strategy which can invade a resident with trait vector  $\mathbf{x}_{\text{res}} = \mathbf{x}^*$ . Write  $\lambda_J$  for the dominant eigenvalue of  $(1/2)(\mathbf{J} + \mathbf{J}^T)$ , the symmetric part of the selection Jacobian, which determines whether  $\mathbf{J}$  is positive/negative definite. Then, we say that  $\mathbf{x}^*$  is convergence stable if  $\lambda_J < 0$ , which means that nearby resident traits  $\mathbf{x}_{\text{res}}$  will evolve towards  $\mathbf{x}^*$ . Conversely, if  $\lambda_J > 0$ , nearby traits  $\mathbf{x}_{\text{res}}$  will evolve away from  $\mathbf{x}^*$ . This allows a classification of the evolutionarily singular points (see Geritz et al., 1998 for a presentation of the simpler case in one-dimensional trait space). In particular,  $\lambda_H < 0$  and  $\lambda_J < 0$  represents a convergence stable ESS (CSS), which serves as a local evolutionary endpoint where no more trait evolution will occur. If  $\lambda_H > 0$  and  $\lambda_J < 0$ ,  $\mathbf{x}^*$  is known as

an evolutionary branching point which initially attracts a monomorphic resident, but where this resident will split into two new morphs that will both diverge away from the branching point.

Here, we have dispensed with several technical subtleties involved in multivariate adaptive dynamics (Leimar, 2001, 2009; Geritz et al., 2016). In particular, we refer to strong convergence stability (sensu Leimar, 2009) simply as convergence stability, and assume that the condition  $\lambda_H > 0, \lambda_J < 0$  will ensure a complete evolutionary branching. This seems to be the case in practice, but has not been completely proven (Geritz et al., 2016).

Before we move on to adaptive dynamics under an implicit trade-off constraint, we will derive one more generic result that will aid us in determining convergence stability. In particular, taking various derivatives with respect to the components of the resident trait vector  $\mathbf{x}_{\text{res}}$  involves the function  $\mathbf{E}(\mathbf{x}_{\text{res}})$  denoting how the equilibrium environment depends on the resident trait. If the ecological model can be solved analytically for arbitrary resident trait vectors, one can just differentiate through the function  $\mathbf{E}(\mathbf{x}_{\text{res}})$ , but this will in general not be possible.

Instead, we define the function  $\mathbf{F}(\mathbf{x}_{\text{res}}, \mathbf{E}) = (\mathbf{f}(\mathbf{x}_{\text{res}}, \mathbf{E}), g(\mathbf{x}_{\text{res}}, \mathbf{E})N)$  and note that in equilibrium  $\mathbf{F}(\mathbf{x}_{\text{res}}, \mathbf{E}) = \mathbf{0}$ . Implicitly differentiating this relationship with respect to  $\mathbf{x}_{\text{res}}$  then yields

$$\frac{\partial \mathbf{E}}{\partial \mathbf{x}_{\text{res}}^T} = - \left( \frac{\partial \mathbf{F}}{\partial \mathbf{E}^T} \right)^{-1} \frac{\partial \mathbf{F}}{\partial \mathbf{x}_{\text{res}}^T}, \quad (8)$$

where the inverse denotes the matrix inverse. Using this we can now calculate

$$\begin{aligned} \frac{\partial^2 \rho(\mathbf{x}, \mathbf{x}_{\text{res}})}{\partial \mathbf{x} \partial \mathbf{x}_{\text{res}}^T} \Big|_{\mathbf{x}=\mathbf{x}_{\text{res}}=\mathbf{x}^*} &= \frac{\partial^2 g(\mathbf{x}, \mathbf{E}(\mathbf{x}_{\text{res}}))}{\partial \mathbf{x} \partial \mathbf{x}_{\text{res}}^T} \Big|_{\mathbf{x}=\mathbf{x}_{\text{res}}=\mathbf{x}^*} = \left[ \frac{\partial^2 g(\mathbf{x}, \mathbf{E})}{\partial \mathbf{x} \partial \mathbf{E}^T} \frac{\partial \mathbf{E}}{\partial \mathbf{x}_{\text{res}}^T} \right]_{\mathbf{x}=\mathbf{x}_{\text{res}}=\mathbf{x}^*} \\ &= - \left[ \frac{\partial^2 g(\mathbf{x}, \mathbf{E})}{\partial \mathbf{x} \partial \mathbf{E}^T} \left( \frac{\partial \mathbf{F}}{\partial \mathbf{E}^T} \right)^{-1} \frac{\partial \mathbf{F}}{\partial \mathbf{x}_{\text{res}}^T} \right]_{\mathbf{x}=\mathbf{x}_{\text{res}}=\mathbf{x}^*}, \end{aligned} \quad (9)$$

which we can subsequently use for calculating the selection Jacobian  $\mathbf{J}$  that determines convergence stability. Note that in taking partial derivatives of  $\mathbf{F}$  w.r.t.  $\mathbf{x}_{\text{res}}$ , the environment  $\mathbf{E}$  is not considered a function of the resident trait vector  $\mathbf{x}_{\text{res}}$ .

## 2.2. Adaptive dynamics under implicit trade-offs

The above presentation assumes that the traits of the trait vector  $\mathbf{x}$  are free to change without constraint. However, typically, trait components cannot vary freely, but are under trade-offs due to, for example, limited time or energy, or physiological limitations. Here, we will consider a single trade-off constraint so that the trait vector has to satisfy  $h(\mathbf{x}) = 0$  (see Fig. 1 for examples). We will say that a trait vector  $\mathbf{x} \in \mathcal{H}$  if  $h(\mathbf{x}) = 0$ , i.e., if  $\mathbf{x}$  is in the trade-off set.

The standard strategy for assuring that a trait vector remains on a trade-off is to find a parameterization  $\theta \in \mathbb{R}^{d-1}$  and let  $\mathbf{x} = \mathbf{x}(\theta)$ . For example, if  $h(\mathbf{x}) = x_1^\alpha + x_2^\alpha - 1$  in  $\mathbb{R}^2$ , we could define

$$\theta \in [0, 1] \subset \mathbb{R}^1, \quad (10a)$$

$$x_1 = \theta^{\frac{1}{\alpha}}, \quad (10b)$$

$$x_2 = (1 - \theta)^{\frac{1}{\alpha}}, \quad (10c)$$

for which one can easily check that  $h(\mathbf{x}(\theta)) \equiv 0$  for all  $\theta \in [0, 1]$ . After this, the  $d - 1$  new traits  $\theta_i$  are free to vary without constraints, and the machinery for evaluating trait evolution presented in the previous section can be used directly for these new traits by defining a new function for the invasion fitness  $\tilde{\rho}(\theta, \theta_{\text{res}}) = \rho(\mathbf{x}(\theta), \mathbf{x}_{\text{res}}(\theta_{\text{res}})) = g(\mathbf{x}(\theta), \mathbf{E}(\mathbf{x}_{\text{res}}(\theta_{\text{res}})))$  and take the appropriate derivatives with respect to  $\theta$  and  $\theta_{\text{res}}$ . While certain parametric trade-offs can be explicitly constructed to be easy to generalize across dimensionalities (Sheftel et al., 2018; Siljestam and Rueffler, 2024), generalizing a specific trade-off described through a parameterization (such as in Eq. (10)) across dimensionalities can be very difficult. Being able to generalize a specific

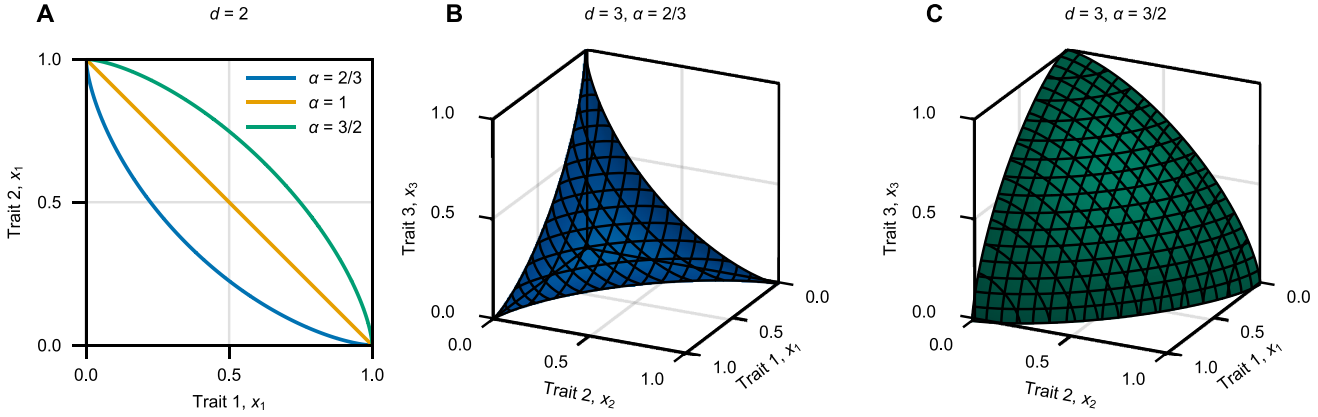


**Fig. 1.** Examples of trade-offs between traits. Each depicted trade-off is defined by  $h(\mathbf{x}) = \sum_{i=1}^d x_i^\alpha - 1 = 0$ . (A) Three different trade-offs in two-dimensional trait space ( $d = 2$ ) defined by  $h(x_1, x_2) = x_1^\alpha + x_2^\alpha - 1 = 0$  for different values of  $\alpha$ . (B) A trade-off in three-dimensional trait space ( $d = 3$ ) defined by  $h(x_1, x_2, x_3) = x_1^\alpha + x_2^\alpha + x_3^\alpha - 1 = 0$  for  $\alpha = 2/3$ . (C) A trade-off in three-dimensional trait space ( $d = 3$ ) defined by  $h(x_1, x_2, x_3) = x_1^\alpha + x_2^\alpha + x_3^\alpha - 1 = 0$  for  $\alpha = 3/2$ .

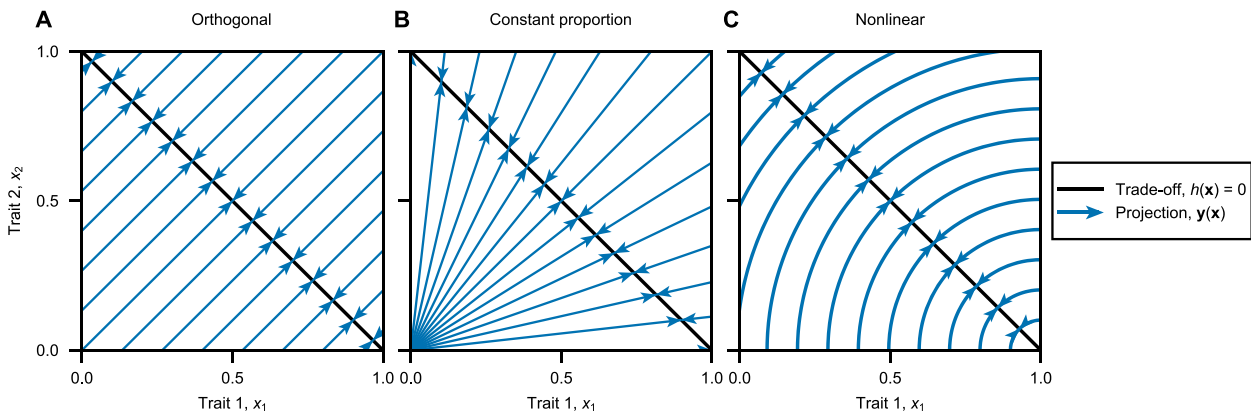


**Fig. 2.** Examples of projection functions  $y$  mapping all traits onto the trade-off set. The black line depicts the trade-off  $h(x_1, x_2) = x_1 + x_2 - 1 = 0$ , and each blue arrow shows all  $\mathbf{x}$  that are mapped onto a specific point on the trade-off under three different projection functions.

trade-off shape is desirable, as a trade-off is often constructed to have certain properties which one would like to retain when generalizing it to higher dimensions. However, parameterizing trade-offs is not necessary to do adaptive dynamics. For example, Ito and Sasaki (2016) used a Lagrange-multiplier formalism to derive expressions for the central first and second-order derivatives used to evaluate directional selection and evolutionary stability.

Here, we will derive an alternative formulation to Ito and Sasaki (2016) and instead of a parameterization use a projection function  $\mathbf{y} : \mathbb{R}^d \rightarrow \mathbb{R}^d$  with the following properties:

$$\mathbf{y}(\mathbf{x}) \in \mathcal{H} \text{ for all } \mathbf{x} \iff h(\mathbf{y}(\mathbf{x})) \equiv 0 \text{ for all } \mathbf{x}, \quad (11a)$$

$$\mathbf{y}(\mathbf{x}) = \mathbf{x} \text{ for all } \mathbf{x} \in \mathcal{H}. \quad (11b)$$

In words, the function  $\mathbf{y}$  maps all trait vectors  $\mathbf{x}$  onto the trade-off set  $\mathcal{H}$ . Just like there are many possible parameterizations of the same trade-off, so too are there many possible projections, see Fig. 2 for examples. We now define a new function  $\tilde{g}(\mathbf{x}, \mathbf{E}) := g(\mathbf{y}(\mathbf{x}), \mathbf{E})$  describing the instantaneous per capita growth rate of a rare morph with trait vector  $\mathbf{x}$  in the environment  $\mathbf{E}$ . Note that since  $\mathbf{y}(\mathbf{x}) = \mathbf{x}$  for all  $\mathbf{x} \in \mathcal{H}$ , for any  $\mathbf{x} \in \mathcal{H}$ ,  $\tilde{g}(\mathbf{x}, \mathbf{E}) = g(\mathbf{x}, \mathbf{E})$ , so the ecological dynamics are unchanged as the trait vectors are assumed to always be on the trade-off set. Similarly, we can express the invasion fitness of a rare invader with trait vector  $\mathbf{x}$  in the environment set by a resident with trait vector  $\mathbf{x}_{\text{res}}$  as  $\tilde{\rho}(\mathbf{x}, \mathbf{x}_{\text{res}}) = \rho(\mathbf{y}(\mathbf{x}), \mathbf{y}_{\text{res}}(\mathbf{x}_{\text{res}}))$ .

Using this together with the chain rule, we can calculate the components of the selection gradient, Hessian, and Jacobian as

$$\tilde{y}_i(\mathbf{x}_{\text{res}}) = \frac{\partial \tilde{g}}{\partial x_i} \Big|_{\mathbf{x}=\mathbf{x}_{\text{res}}} = \left[ \sum_{k=1}^d \frac{\partial y_k}{\partial x_i} \frac{\partial g}{\partial y_k} \right]_{\mathbf{y}=\mathbf{x}=\mathbf{x}_{\text{res}}}, \quad (12a)$$

$$\begin{aligned} \tilde{H}_{ij} &= \frac{\partial^2 \tilde{g}}{\partial x_i \partial x_j} \Big|_{\mathbf{x}=\mathbf{x}_{\text{res}}=\mathbf{x}^*} \\ &= \left[ \sum_{k=1}^d \frac{\partial^2 y_k}{\partial x_i \partial x_j} \frac{\partial g}{\partial y_k} + \sum_{k=1}^d \sum_{l=1}^d \frac{\partial y_k}{\partial x_i} \frac{\partial^2 g}{\partial y_k \partial y_l} \frac{\partial y_l}{\partial x_j} \right]_{\mathbf{y}=\mathbf{y}^*=\mathbf{x}=\mathbf{x}_{\text{res}}=\mathbf{x}^*}, \end{aligned} \quad (12b)$$

$$\begin{aligned} \tilde{J}_{ij} &= \tilde{H}_{ij} + \frac{\partial^2 \tilde{g}}{\partial x_i \partial x_j^{\text{res}}} \Big|_{\mathbf{x}=\mathbf{x}_{\text{res}}=\mathbf{x}^*} \\ &= \tilde{H}_{ij} + \left[ \sum_{k=1}^d \sum_{l=1}^d \frac{\partial y_k}{\partial x_i} \frac{\partial^2 g}{\partial y_k \partial y_l^{\text{res}}} \frac{\partial y_l^{\text{res}}}{\partial x_j} \right]_{\mathbf{y}=\mathbf{y}^*=\mathbf{x}=\mathbf{x}_{\text{res}}=\mathbf{x}^*}. \end{aligned} \quad (12c)$$

At first blush, this maneuver seems not to have served any particularly useful purpose as we now have to come up with a projection function  $\mathbf{y}(\mathbf{x})$ , which does not appear to be any easier than coming up with a parameterization  $\mathbf{x}(\theta)$ . Coming up with a good projection is occasionally possible. For example, the well-known replicator equations (see e.g., Cressman and Tao 2014) use the projection  $\mathbf{y}(\mathbf{x}) = (1 / \sum_{j=1}^d x_j) \mathbf{x}$  for the trade-off  $h(\mathbf{x}) = \sum_{i=1}^d x_i - 1 = 0$  (see Fig. 2B) to track changes in proportions (frequencies). In general, however, coming up with a generic method for constructing a good projection  $\mathbf{y}$  from an arbitrary

trade-off  $h$  seems to be as difficult as coming up with a generic method for constructing parameterizations.

The first key insight to use the projections is that a full specification of  $y$  is not necessary. Looking at Eq. (12), we see that only the first and second derivatives evaluated on the trade-off are necessary to evaluate the selection gradient, Hessian, and Jacobian. The second is that we can get direct conditions for these derivatives by using the fact that  $h(y(x)) \equiv 0$  for all  $x \in \mathbb{R}^d$ , since  $y$  projects all  $x$  onto the trade-off set. Since the function is identically equal to zero, so must its derivatives also be. Taking derivatives, we thus get the equations

$$h(y(x)) = 0 \text{ for all } x, \quad (13a)$$

$$\frac{\partial h}{\partial x_i} = \sum_{k=1}^d \frac{\partial h}{\partial y_k} \frac{\partial y_k}{\partial x_i} = 0 \text{ for all } x, \quad (13b)$$

$$\frac{\partial^2 h}{\partial x_i \partial x_j} = \sum_{k=1}^d \frac{\partial^2 y_k}{\partial x_i \partial x_j} \frac{\partial h}{\partial y_k} + \sum_{k=1}^d \sum_{l=1}^d \frac{\partial y_k}{\partial x_i} \frac{\partial^2 h}{\partial y_k \partial y_l} \frac{\partial y_l}{\partial x_j} = 0 \text{ for all } x. \quad (13c)$$

In addition, the condition  $y(x) = x$  for  $x \in \mathcal{H}$  translates locally into the condition

$$\sum_{i=1}^d \frac{\partial y_k}{\partial x_i} u_i = u_k \text{ for all } u \perp \frac{\partial h(x)}{\partial x}. \quad (14)$$

Writing  $P := \partial y / \partial x^T$  (with entries  $P_{ij} = \partial y_i / \partial x_j$ ) for the local projection matrix, these conditions state that the gradient of the constraint  $\nabla h = \partial h(x) / \partial x$  should be a left eigenvector of the projection matrix  $P$  with eigenvalue zero, and that any vector  $u$  orthogonal to  $\nabla h$  should be a right eigenvector of the projection matrix  $P$  with eigenvalue one.

Just as the same trade-off can be parameterized in many different ways and there are many forms of  $y(x)$  that project onto the same trade-off (Fig. 2), there are many local descriptions through the derivatives of  $y$  that will satisfy Eqs. (13) and (14). And just as we would have little to go on in terms of empirical data for parameterizing a trade-off, we know of no empirical studies that could aid us in picking a local projection. However, one local description that stands out as mathematically natural is local orthogonal projection onto the trade-off. For the remainder of this paper, we will use local orthogonal projection, so that around every point on the trade-off curve, nearby points are projected along the direction perpendicular to the trade-off, as in Fig. 2A. To help write down the formulas, we write

$$h_i := \frac{\partial h}{\partial y_i} \Big|_{y=x}, \quad (15a)$$

$$h_{ij} := \frac{\partial^2 h}{\partial y_i \partial y_j} \Big|_{y=x}, \quad (15b)$$

which we can use to formulate an expression for local orthogonal projection:

$$\frac{\partial y_k}{\partial x_i} = \delta_{ki} - \frac{h_k h_i}{\sum_{l=1}^d (h_l)^2}, \quad (16)$$

where  $\delta_{ki}$  is the Kronecker delta. On the trade-off, one can easily check that this form of  $\partial y_k / \partial x_i$  satisfies Eqs. (13b) and (14). We thus have that the selection gradient is given by

$$\tilde{\gamma}_i(x_{\text{res}}) = \left[ \sum_{k=1}^d \left( \delta_{ki} - \frac{h_k h_i}{\sum_{l=1}^d (h_l)^2} \right) \frac{\partial g}{\partial y_k} \right]_{y=y_{\text{res}}=x=x_{\text{res}}}. \quad (17)$$

That this would work is, perhaps, no surprise: if we remove the component of the raw selection gradient that is perpendicular to the trade-off set, then directional selection will proceed along the trade-off; see Fig. 3 for an example.

Choosing this expression for  $\partial y_k / \partial x_i$ , one can then check that an expression for the second derivatives  $\partial^2 y_k / \partial x_i \partial x_j$  satisfying Eq. (13c) is given by

$$\frac{\partial^2 y_k}{\partial x_i \partial x_j} = \frac{1}{\sum_{m=1}^d (h_m)^2} (h_{kj} h_i + h_{ki} h_j - h_{ij} h_k) - \frac{1}{(\sum_{m=1}^d (h_m)^2)^2} \sum_{l=1}^d h_{kl} h_l h_i h_j. \quad (18)$$

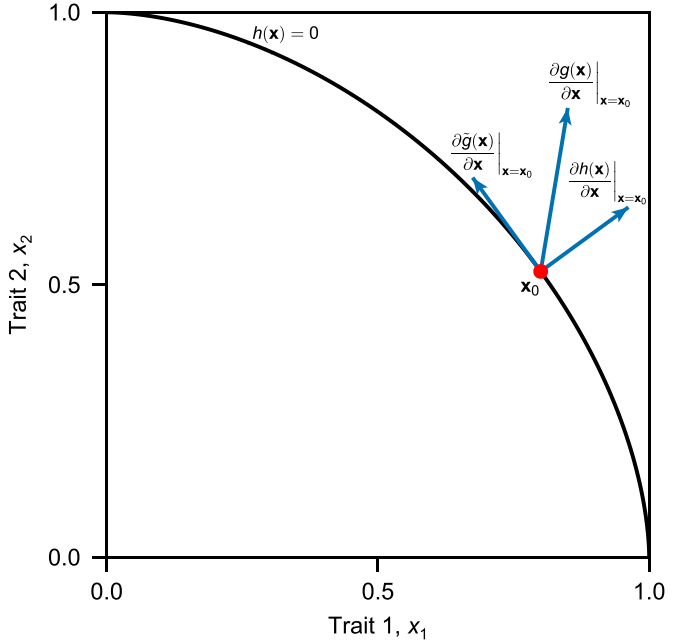


**Fig. 3.** Example of projection of the raw selection gradient onto a trade-off. The raw selection gradient  $\partial g(x) / \partial x|_{x=x_0}$  at a point  $x_0$  describes what the direction of maximal fitness increase would have been without a trade-off constraint  $h(x) = 0$ . The raw selection gradient is projected orthogonally onto the trade-off to yield the realized selection gradient  $\partial \tilde{g}(x) / \partial x|_{x=x_0} = \hat{\gamma}(x_0)$  by removing the component of  $\partial g(x) / \partial x|_{x=x_0}$  in the direction of the gradient of the trade-off,  $\partial h(x) / \partial x|_{x=x_0}$ .

This expression does not easily lend itself to intuitive interpretation. One important property of this locally defined projection is that it makes any function of  $y(x)$  flat in the direction of  $\nabla h$  (the direction orthogonal to the trade-off set). Thus, the matrices  $\bar{H}$  and  $\bar{J}$  will always have a zero eigenvalue associated with the eigenvector  $\nabla h$ . This means that we have to amend our definitions of evolutionary and convergence stability. Thus, we let  $\lambda_{\bar{H}}$  be the largest eigenvalue of  $\bar{H}$  that is not associated with the eigenvector  $\nabla h$ , and let  $\lambda_J$  be the largest eigenvalue of  $(1/2)(\bar{J} + \bar{J}^T)$  not associated with the eigenvector  $\nabla h$ . As one might expect, our projection has reduced the effective dimensionality by one, just as a parameterization would have. The matrices  $\bar{H}$  and  $\bar{J}$  are still matrices in the unconstrained trait space, and if, for example,  $\bar{H}$  has a single positive eigenvalue, the associated eigenvector tells the direction along which the resident can be invaded in the unconstrained space (the branching direction if  $x^*$  is convergence stable), but this direction will necessarily be in the tangent (hyper-)plane of the trade-off set.

Finally, we need to amend our expression using implicit differentiation for evaluating the derivatives with respect to the resident trait vector, Eq. (9). Once again using the chain rule, this can be evaluated to be

$$\frac{\partial^2 \rho(x, x_{\text{res}})}{\partial x \partial x_{\text{res}}^T} = - \left[ \frac{\partial y^T}{\partial x} \frac{\partial^2 g}{\partial y \partial E^T} \left( \frac{\partial F}{\partial E^T} \right)^{-1} \frac{\partial F}{\partial y_{\text{res}}^T} \frac{\partial y_{\text{res}}^T}{\partial x_{\text{res}}^T} \right]_{y=y_{\text{res}}=x=x_{\text{res}}=x^*}. \quad (19)$$

Using the expressions for the derivatives of  $y(x)$  in Eqs. (16) and (18), we see that the expressions for the selection gradient, Hessian, and Jacobian (Eq. (12)) are fully expressed in terms of the known functions  $g$  and  $h$ , and we can thus carry out standard adaptive-dynamics analyses for any (sufficiently smooth) systems described in terms of a per capita growth function  $g$  and an implicitly defined trade-off  $h$ . In Table 1 we collect all the definitions and expressions that are necessary for carrying out such analyses.

**Table 1**

Symbols, variables, and formulas for carrying out adaptive dynamics under implicit trade-offs.

Symbol	Definition	Expression/note
$d$	Trait space dimensionality	
$\mathbf{x}$	Trait vector	$\mathbf{x} = (x_1, x_2, \dots, x_d)$
$\mathbf{E}'$	Vector of environmental factors	
$N$	Species density	
$\mathbf{E}$	Environment	$\mathbf{E} = (\mathbf{E}', N)$
$g(\mathbf{x}, \mathbf{E})$	Per capita growth rate of rare morph with trait vector $\mathbf{x}$	$\mathbf{x} \in \mathcal{H} \iff \mathbf{x}$ is on the trade-off
$\mathcal{H}$	Trade-off set	$h(\mathbf{x}) = 0 \iff \mathbf{x} \in \mathcal{H}$
$h(\mathbf{x})$	Implicit trade-off function	$y(\mathbf{x}) \in \mathcal{H} \forall \mathbf{x}, y(\mathbf{x}) = \mathbf{x} \forall \mathbf{x} \in \mathcal{H}$
$y(\mathbf{x})$	Projection function onto trade-off	
$h_k$	Gradient of $h$	$h_k = \frac{\partial h}{\partial y_k} \Big _{\mathbf{y}=\mathbf{x}}$
$h_{kl}$	Hessian of $h$	$h_{kl} = \frac{\partial^2 h}{\partial y_k \partial y_l} \Big _{\mathbf{y}=\mathbf{x}}$
$\frac{\partial y_k}{\partial x_i}$	First derivatives of projection on $\mathcal{H}$	$\frac{\partial y_k}{\partial x_i} = \delta_{ik} - \frac{h_k h_{ki}}{\sum_{j=1}^d (h_j)^2}$
$\frac{\partial^2 y_k}{\partial x_i \partial x_j}$	Second derivatives of projection on $\mathcal{H}$	$\frac{\partial^2 y_k}{\partial x_i \partial x_j} = \frac{1}{\sum_{m=1}^d (h_m)^2} (h_{kj} h_i + h_{ki} h_j - h_{ij} h_k) - \frac{1}{\sum_{m=1}^d (h_m)^4} \sum_{l=1}^d h_{kl} h_l h_i h_j$
$\mathbf{x}_{\text{res}}$	Resident trait vector	$g(\mathbf{x}_{\text{res}}, \mathbf{E}(\mathbf{x}_{\text{res}})) = 0$
$\rho(\mathbf{x}, \mathbf{x}_{\text{res}})$	Invasion fitness of morph with trait vector $\mathbf{x}$ into environment set by resident with trait vector $\mathbf{x}_{\text{res}}$	$\rho(\mathbf{x}, \mathbf{x}_{\text{res}}) = g(\mathbf{x}, \mathbf{E}(\mathbf{x}_{\text{res}}))$
$\gamma(\mathbf{x}_{\text{res}})$	Selection gradient	$\gamma(\mathbf{x}_{\text{res}}) = \frac{\partial \rho(\mathbf{x}, \mathbf{x}_{\text{res}})}{\partial \mathbf{x}} \Big _{\mathbf{x}=\mathbf{x}_{\text{res}}} \quad \gamma(\mathbf{x}^*) = 0$
$\mathbf{x}^*$	Evolutionarily singular point	$\mathbf{H}_{ij} = \frac{\partial^2 \rho(\mathbf{x}, \mathbf{x}_{\text{res}})}{\partial x_i \partial x_j} \Big _{\mathbf{x}=\mathbf{x}_{\text{res}}=\mathbf{x}^*}$
$\mathbf{H}_{ij}$	Selection Hessian	$J_{ij} = \frac{\partial^2 \rho(\mathbf{x}, \mathbf{x}_{\text{res}})}{\partial x_i \partial x_j} \Big _{\mathbf{x}=\mathbf{x}_{\text{res}}=\mathbf{x}^*} + \frac{\partial^2 \rho(\mathbf{x}, \mathbf{x}_{\text{res}})}{\partial x_i \partial x_j^{\text{res}}} \Big _{\mathbf{x}=\mathbf{x}_{\text{res}}=\mathbf{x}^*}$
$J_{ij}$	Selection Jacobian	$\tilde{g}(\mathbf{x}, \mathbf{E}) = g(y(\mathbf{x}), \mathbf{E})$
$\tilde{g}(\mathbf{x}, \mathbf{E})$	Per capita growth rate under trade-off	$\tilde{\rho}(\mathbf{x}, \mathbf{x}_{\text{res}}) = \tilde{g}(\mathbf{x}, \mathbf{E}(\mathbf{x}_{\text{res}})) = \rho(y(\mathbf{x}), y_{\text{res}}(\mathbf{x}_{\text{res}}))$
$\tilde{\rho}(\mathbf{x}, \mathbf{x}_{\text{res}})$	Invasion fitness under trade-off	$\tilde{\gamma}_i(\mathbf{x}_{\text{res}}) = \frac{\partial \tilde{\rho}}{\partial x_i} \Big _{\mathbf{x}=\mathbf{x}_{\text{res}}} = \frac{\partial \tilde{g}}{\partial x_i} \Big _{\mathbf{x}=\mathbf{x}_{\text{res}}} = \sum_{k=1}^d \frac{\partial y_k}{\partial x_i} \frac{\partial g}{\partial y_k} \Big _{\mathbf{y}=y_{\text{res}}=\mathbf{x}=\mathbf{x}_{\text{res}}}$
$\tilde{\gamma}(\mathbf{x}_{\text{res}})$	Selection gradient under trade-off	$\tilde{\mathbf{H}}_{ij} = \frac{\partial^2 \tilde{\rho}}{\partial x_i \partial x_j} \Big _{\mathbf{x}=\mathbf{x}_{\text{res}}=\mathbf{x}^*}$
$\tilde{\mathbf{H}}_{ij}$	Selection Hessian under trade-off	$= \left[ \sum_{k=1}^d \frac{\partial^2 y_k}{\partial x_i \partial x_k} \frac{\partial g}{\partial y_k} + \sum_{k=1}^d \sum_{l=1}^d \frac{\partial y_k}{\partial x_i} \frac{\partial^2 g}{\partial y_k \partial y_l} \frac{\partial y_l}{\partial x_j} \right]_{\mathbf{y}=y^{\text{res}}=\mathbf{x}=\mathbf{x}_{\text{res}}=\mathbf{x}^*}$
$\tilde{J}_{ij}$	Selection Jacobian under trade-off	$\tilde{J}_{ij} = \frac{\partial^2 \tilde{g}}{\partial x_i \partial x_j} \Big _{\mathbf{x}=\mathbf{x}_{\text{res}}=\mathbf{x}^*} + \frac{\partial^2 \tilde{g}}{\partial x_i \partial x_j^{\text{res}}} \Big _{\mathbf{x}=\mathbf{x}_{\text{res}}=\mathbf{x}^*}$
$\lambda_H$	Determinant of evolutionary stability of $\mathbf{x}^*$	$= \tilde{\mathbf{H}}_{ij} + \left[ \sum_{k=1}^d \sum_{l=1}^d \frac{\partial y_k}{\partial x_i} \frac{\partial^2 g}{\partial y_k \partial y_l} \frac{\partial y_l}{\partial x_j^{\text{res}}} \right]_{\mathbf{y}=y^{\text{res}}=\mathbf{x}=\mathbf{x}^{\text{res}}=\mathbf{x}^*}$
$\lambda_J$	Determinant of convergence stability of $\mathbf{x}^*$	Dominant eigenvalue of $\tilde{\mathbf{H}}$ not associated with the eigenvector $\nabla h(\mathbf{x}^*)$ $\lambda_H < 0 \implies$ evolutionarily stable, $\lambda_H > 0 \implies$ not evolutionarily stable Dominant eigenvalue of $\frac{1}{2}(J + J')$ not associated with the eigenvector $\nabla h(\mathbf{x}^*)$ $\lambda_J < 0 \implies$ convergence stable, $\lambda_J > 0 \implies$ not convergence stable

### 3. Examples

We will now turn to applying our above-derived expressions to two models of resource competition, one very simple and the other more elaborate. In particular, we will examine the stability characteristics of the evolutionarily singular point where a generalist consumer is equally invested in consuming all  $d$  resources, and investigate how diverse a community can be attained through adaptive radiations through successive evolutionary branching for different number of resources and different trade-off shapes.

#### 3.1. Example 1: a simple resource-competition model

Our first example model builds on classic eco-evolutionary resource-competition models for two resources (Lawlor and Smith, 1976; Rueffler et al., 2006) and is simple enough that we can derive some results analytically. A very similar model with  $d$  resources was studied by Caetano et al. (2021), but due to an approximation they made to derive analytical results, their findings differ qualitatively from what we will describe here. We consider a single consumer species with density  $N$  and with trait vector  $\mathbf{x}$ , where each component  $x_i$  describes the affinity for substitutable resource  $R_i$ ,  $i = 1, \dots, d$ . The uptake affinities are constrained by a trade-off  $h(\mathbf{x}) = 0$  so that a consumer can only get better at taking up one resource at the expense of its ability to take up others, see Fig. 1 for examples for  $d = 2$  and  $d = 3$ . The model is given by

$$g(\mathbf{x}, \mathbf{E}) = \sum_{i=1}^d x_i R_i - m, \quad (20a)$$

$$h(\mathbf{x}) = \sum_{i=1}^d x_i^\alpha - 1, \quad (20b)$$

$$\frac{dN}{dt} = g(\mathbf{x}_{\text{res}}, \mathbf{E})N, \quad (20c)$$

$$\frac{dR_i}{dt} = r(K - R_i) - x_i^{\text{res}} R_i N, \quad (20d)$$

$$\mathbf{E} = (\mathbf{R}, N) = (R_1, R_2, \dots, R_d, N). \quad (20e)$$

Here, the consumer grows according to a type-I functional response, and suffers a constant background mortality  $m$ . To keep the model analytically tractable, we assume a highly symmetric resource configuration, where each resource is renewed chemostatically at rate  $r$  from a supply with concentration  $K$ , which we take to be the same for all resources. We assume that the conversion efficiency of resources into consumers equals one for all resources. Using chemostat dynamics also ensure that the ecological dynamics of the model always reaches an equilibrium. Our general expressions for evaluating selection (Table 1) would work equally well for biotic resources described by, for example, logistic growth, as long as the ecological dynamics do not exhibit limit cycles (as may be the case in classic predator-prey models; Rosenzweig and MacArthur 1963).

Since we assume that  $x_i$  describes the affinity of the consumer for resource  $i$ , we must in addition to the trade-off  $h(\mathbf{x}) = 0$  assume that each  $x_i$  satisfies  $x_i \geq 0$ . Note that the trade-off itself implicitly imposes the constraint  $x_i \leq 1$  for all  $i$ . Our general machinery for adaptive dynamics under constraints strictly speaking only applies to the interior of the trade-off set, but we will here extend this in the obvious way to the boundary, and say, for example, that a trait vector  $\mathbf{x}^*$  is an ESS if it is on

the boundary and no nearby points on the boundary or in the interior of the trade-off set have positive invasion fitness (a boundary ESS).

The global trait dynamics of this system are simple. For generalist-favoring trade-offs ( $\alpha > 1$ , for example Fig. 1C), a single generalist consumer with equal affinity for all resources is globally uninvasive by any other trait combination on the trade-off. For specialist-favoring trade-offs ( $\alpha < 1$ , for example Fig. 1B), a community of  $d$  consumers, each fully specialized on a single resource is globally uninvasive by any other trait combination (Supplementary S1.1). These would be the outcomes if all of trait space was accessible, for example due to low levels of immigration where immigrants could have any feasible trait vector. Below, we will explore the case where consumers are only allowed to evolve through small mutations in an adaptive radiation, which would be the case, for example, if an island was colonized through a single rare migration event. Under these assumptions, there may be niches that remain unoccupied due to fitness valleys that cannot be bridged through small mutations.

All calculations of quantities for evaluating the evolutionary behavior requires that we calculate the gradient and Hessian of the trade-off function  $h$ , which are given by

$$h_k = \alpha x_k^{\alpha-1}, \quad (21a)$$

$$h_{kl} = \alpha(\alpha-1)x_k^{\alpha-2}\delta_{kl}. \quad (21b)$$

We can then calculate the selection gradient by first calculating the first derivative of the projection function

$$\frac{\partial y_k}{\partial x_i} = \delta_{ki} - \frac{h_k h_i}{\sum_{l=1}^d (h_l)^2} = \delta_{ki} - \frac{x_k^{\alpha-1} x_i^{\alpha-1}}{\sum_{l=1}^d x_l^{2(\alpha-1)}} \quad (22)$$

and the gradient of  $g$ ,  $g_i = R_i$ , giving

$$\tilde{y}_i(x_{\text{res}}) = \sum_{k=1}^d \frac{\partial y_k}{\partial x_i} \frac{\partial g}{\partial y_k} \Big|_{y=x=x_{\text{res}}} = \sum_{k=1}^d \left( \delta_{ki} - \frac{x_k^{\alpha-1} x_i^{\alpha-1}}{\sum_{l=1}^d x_l^{2(\alpha-1)}} \right) \Big|_{x=x_{\text{res}}} R_k(x_{\text{res}}). \quad (23)$$

Based on the symmetry of the system, we can guess that the trait vector  $x^*$  where all components are equal is an evolutionarily singular point, which when solved from the trade-off yields  $x_i^* = x^* = (1/d)^{1/\alpha}$ . From this, we can solve for the full eco-evolutionary equilibrium

$$x_i^* = x^* = \left( \frac{1}{d} \right)^{\frac{1}{\alpha}} \text{ for all } i = 1, \dots, d, \quad (24a)$$

$$R_i^* = R^* = \frac{m}{dx^*} \text{ for all } i = 1, \dots, d, \quad (24b)$$

$$N^* = \frac{rd}{m} \left( K - \frac{m}{dx^*} \right). \quad (24c)$$

Inserting these expressions into the expression for the selection gradient reveals that

$$\tilde{y}_i(x^*) = \sum_{k=1}^d \left( \delta_{ik} - \frac{1}{d} \right) R^* = \left( 1 - \frac{d}{d} \right) R^* = 0, \quad (25)$$

so that  $x^*$  is indeed an evolutionarily singular point. At the singular point  $x^*$  we can calculate the entries of the first derivatives of the projection function  $P_{ki} = \partial y_k / \partial x_i |_{x=x^*}$  by inserting  $x_i^* = x^* = (1/d)^{1/\alpha}$  into Eq. (22), which when put into matrix form yields

$$P := \frac{\partial y}{\partial x^T} \Big|_{x=x^*} = \begin{bmatrix} 1 - 1/d & -1/d & \dots & -1/d \\ -1/d & 1 - 1/d & \dots & -1/d \\ \vdots & \vdots & \ddots & \vdots \\ -1/d & -1/d & \dots & 1 - 1/d \end{bmatrix}. \quad (26)$$

This projection matrix (in the linear-algebra sense) has two distinct eigenvalues, zero and one, with the eigenvalue being zero in the  $(1, 1, \dots, 1) \propto \nabla h(x^*)$  direction, and one for any direction perpendicular to this direction. Now, using the expressions from Table 1 together with the expressions for the equilibrium values for the system (Eq. (24)) we

can calculate the selection Hessian and Jacobian to be (Supplementary S1.2)

$$\tilde{H} = (1 - \alpha) \frac{R^*}{x^*} P, \quad (27a)$$

$$J = \left( \frac{m}{K} d^{\frac{1-\alpha}{\alpha}} - \alpha \right) \frac{R^*}{x^*} P, \quad (27b)$$

which due to the simple eigenstructure of  $P$  means that

$$\lambda_{\tilde{H}} = (1 - \alpha) \frac{R^*}{x^*}, \quad (28a)$$

$$\lambda_J = \left( \frac{m}{K d x^*} - \alpha \right) \frac{R^*}{x^*} = \left( \frac{m}{K} d^{\frac{1-\alpha}{\alpha}} - \alpha \right) \frac{R^*}{x^*}. \quad (28b)$$

The evolutionarily singular point  $x^*$  is evolutionarily stable ( $\lambda_{\tilde{H}} < 0$ ) whenever  $\alpha > 1$ , which is simply a function of the curvature of the trade-off (see Fig. 1 for examples), and does not depend on the dimensionality of the system.

The conditions for convergence stability ( $\lambda_J < 0$ ) are more interesting. First, in order for the consumer to persist it must hold that  $K > m/(dx^*)$  (Eq. (24c)), which in turn means that  $m/(K d x^*) < 1$ , so whenever  $\alpha > 1$ ,  $x^*$  is convergence stable, and thus evolutionary stability implies convergence stability (no ‘garden of Eden’ sensu Geritz et al. 1998). When  $\alpha < 1$ , the evolutionarily singular point may or may not be convergence stable. For a given dimensionality  $d$ , the critical  $\alpha$  yielding  $\lambda_J = 0$  is given by the equation  $\alpha_{\text{crit}} = \ln d / W((Kd/m)\ln d)$ , where  $W$  is Lambert’s  $W$  function, and with convergence stability being attained for  $\alpha > \alpha_{\text{crit}}$ . Conversely, for a given  $\alpha$ , convergence stability is attained if  $d < (\alpha K/m)^{\alpha/(1-\alpha)}$ . This means that if  $x^*$  is convergence stable for dimensionality  $d$ , it will also be convergence stable for  $d-1$ ,  $d-2$ , and so on, when other parameter values are kept fixed.

These properties of the evolutionarily singular point have some interesting implications for adaptive radiations in the model. If a consumer in a system with  $d$  resources has a trait vector where one of the  $d$  trait components is zero, say for resource  $j$ , then this means that resource  $j$  is not participating in the system anymore and the trait space is now effectively of dimensionality  $d-1$ , with the trade-off among the remaining  $d-1$  resource affinities being exactly the same as the trade-off specified for a dimensionality of  $d-1$ . For a  $d$ -dimensional system where the central evolutionarily singular point  $x^* = (x^*, x^*, \dots, x^*)$  is convergence stable but not evolutionarily stable this will result in an evolutionary branching where we get two new species evolving away from the original singular point. If these species then evolve to a new singular point where the species do not share resources, these new singular points would also be branching points since their dimensionality will be lower than the original central evolutionarily singular point. This suggests that if the  $d$ -dimensional central singular point  $x^* = (x^*, x^*, \dots, x^*)$  is a branching point, a complete radiation filling all niche space is possible, where the final result is one fully specialized consumer for each resource. However, our analysis here is only local around the branching point and whether a complete radiation will occur depends on the global basins of attraction of the various lower-dimensional subsequent evolutionarily singular points, which we cannot determine analytically.

To get a better appreciation for the behavior of the model we simulate the eco-evolutionary dynamics by adding an equation for the trait evolution to Eq. (20):

$$\frac{dx_i^{\text{res}}}{dt} = \epsilon_{\text{evo}} \tilde{y}_i(x_{\text{res}}), \quad (29)$$

where  $\epsilon_{\text{evo}}$  is some small number separating ecological and evolutionary timescales, so that all species evolve their traits in the direction of the selection gradient, taking the trade-off into account. Starting with a single species, we first let this species evolve to an evolutionarily singular point. We then check if the evolutionarily singular point is an evolutionary branching point, and if so, split the species into two new species in the direction of maximum curvature (the eigenvector associated with  $\lambda_{\tilde{H}}$ ). We repeat this process until all residents are locally stable. We depict two such assembly processes for  $d = 3$  in Fig. 4.

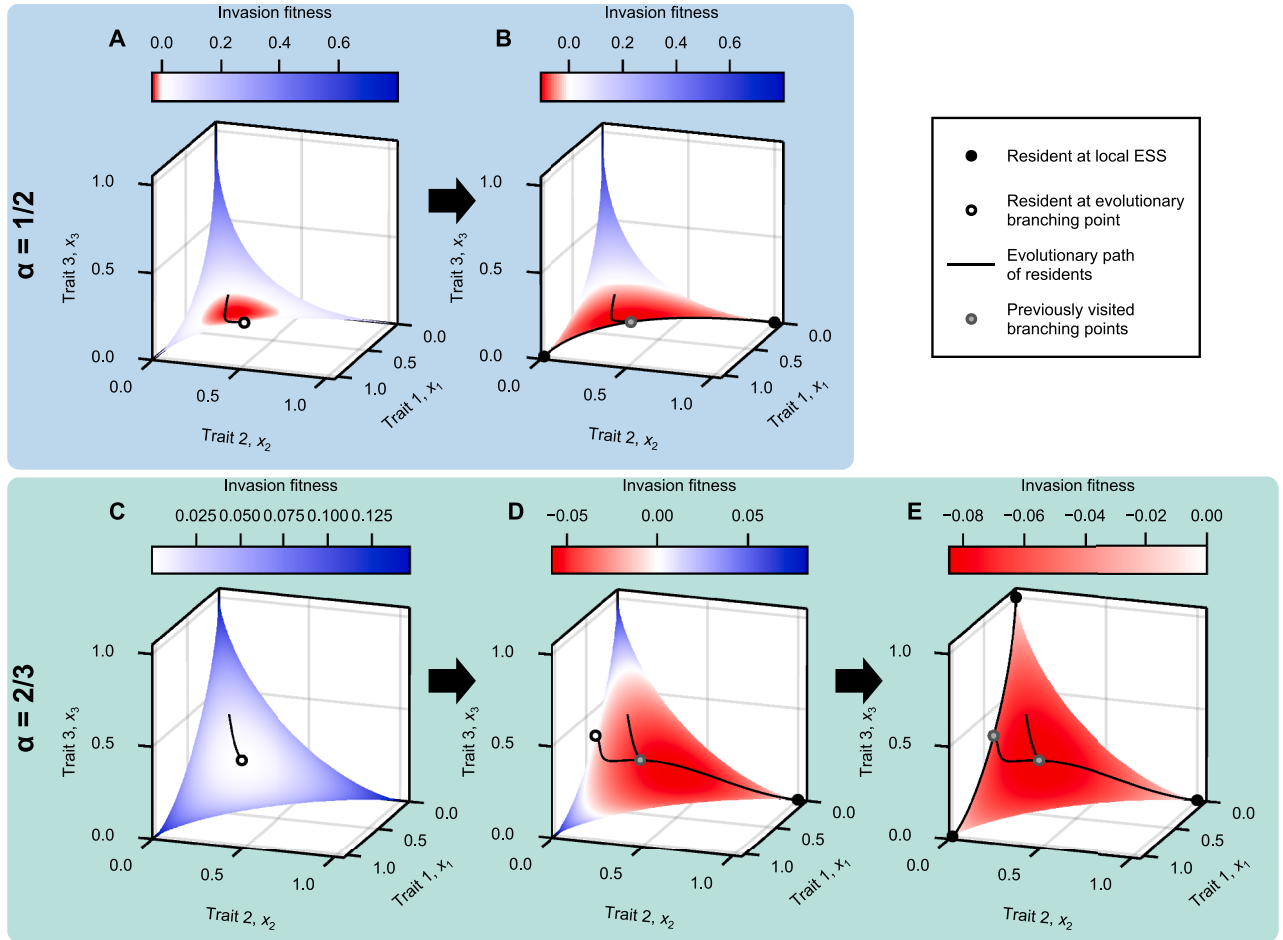


**Fig. 4.** Examples of eco-evolutionary community assembly for the simple resource-competition model (Eq. (20)). Two different community-assembly outcomes (A–B with  $\alpha = 1/2$  and C–E with  $\alpha = 2/3$ ) are depicted. Each panel shows the residents (black dots) at an evolutionarily singular point with the residents' paths through trait space shown as black lines. For the given configuration of residents, the invasion-fitness landscape for rare mutants is depicted as a color gradient on the trade-off surface. Other parameters:  $r = 1$ ,  $K = 1$ ,  $m = 0.2$ .

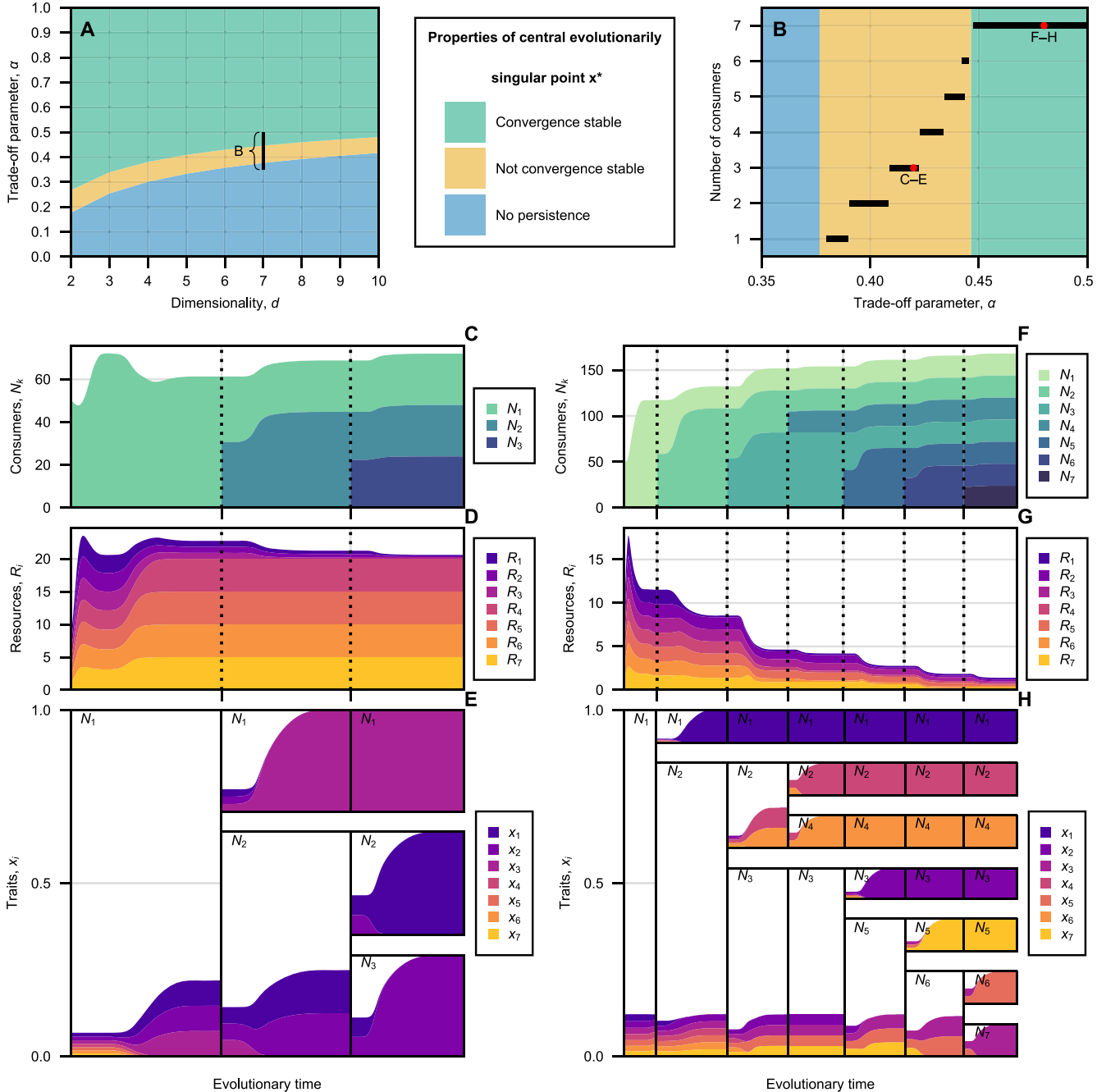
Fig. 4A and B shows the assembly process when the central evolutionarily singular point is a repeller. Thus, even starting close to the evolutionarily singular point, the resident evolves away from the center until it reaches a singular point with  $x_3 = 0$  (Fig. 4A). While this is a fitness maximum in the  $x_3$ -direction, it is a fitness minimum in the  $x_1-x_2$  direction, and the resident splits into two new species. These then evolve until they both reach evolutionarily singular points with one complete resource-one specialist and one complete resource-two specialist (Fig. 4B). This two-species community is locally stable as no invader with traits close to either resident can invade, and the community cannot become further diversified through evolutionary branching. It is, however, not globally stable, as any invader sufficiently specialized on resource three could invade, as indicated by the fitness landscape (Fig. 4B).

Fig. 4C–E shows an example of the assembly process for  $d = 3$  when the central singular point is a branching point. Here, the single resident initially evolves to the central evolutionarily singular point, and ends up at a global fitness minimum (Fig. 4C). After branching, the two new residents end up at a branching point and an ESS respectively (Fig. 4D). The resident with  $x_2 = 0$  subsequently branches, and the final outcome is a community where each resident fully specializes on one resource (Fig. 4E).

To get a better sense of when adaptive radiations can yield fully saturated communities, we combine our analytical results for the properties of the central evolutionarily singular point  $\mathbf{x}^* = (x_1^*, \dots, x_d^*)$  with numer-

ical simulations in seven-dimensional trait space (Fig. 5). We depict the properties we derived analytically for  $\mathbf{x}^*$  in Fig. 5A, which shows how increasing dimensionality reduces the range of trade-off shapes  $\alpha$  that yield convergence stability for  $\mathbf{x}^*$ . For  $d = 7$ , we numerically assemble communities through successive evolutionary branching (as in Fig. 4) until all residents are at a local ESS and where the initial conditions are a point not exactly on but very close to the central evolutionarily singular point  $\mathbf{x}^*$ . We depict the number of consumers in the final community in Fig. 5B. Depicting eco-evolutionary trajectories in seven-dimensional trait space is not straight-forward, but we show two examples of assembly through successive branching in Fig. 5C–E and F–H respectively. The evolution of the traits (Fig. 5E, H) is depicted as a series of branching panels, wherein each panel the trait composition over time for a single consumer is depicted. At each evolutionary-branching event, the panel of the branching consumer is split into two new panels.

When  $\mathbf{x}^*$  is convergence stable, the assembly procedure does result in a fully saturated community with seven residents, each fully specialized on one resource (Fig. 5B, see Fig. 5F–H for an example). For the range of  $\alpha$  where  $\mathbf{x}^*$  is not convergence stable, several species may still evolve, with lower values of  $\alpha$  yielding fewer species in the final community (Fig. 5B). Comparing Figs. 5A and B, we see that the pattern is not so simple as to merely reflect the maximal dimensionality for which  $\mathbf{x}^*$  is convergence stable. For  $\alpha = 0.4$ , for example, only two species emerge from the radiation in  $d = 7$  (Fig. 5B), while



**Fig. 5.** Behavior of central evolutionarily singular point and adaptive radiations for Example 1. (A) Characteristics of the central singular point  $x_i^* = (1/d)^{1/\alpha}$  for  $i = 1, \dots, d$  for different dimensionalities  $d$  and trade-off parameters  $\alpha$ . The black line indicates the span of  $\alpha$ s for  $d = 7$  shown in panel B. (B) Number of consumers assembled numerically through successive evolutionary branching for initial conditions close to  $x^*$  for  $d = 7$  and different trade-off parameters  $\alpha$ . The two red dots indicate the values of  $\alpha$  for two outcomes shown in greater detail in panels C–E and F–H respectively. (C–E) Community assembly through successive evolutionary branching. The panels show the density of consumers (C), the density of resources (D), and the traits of each consumer (E). (F–H) Same as C–E, but for a different trade-off parameter  $\alpha$  (see panel B). Other parameters:  $r = 1$ ,  $K = 5$ ,  $m = 0.2$ .

the maximal dimensionality for which  $x^*$  is stable is  $d = 4$  (Fig. 5A). In general, our numerical experiments indicate that the final community seems to contain as many consumers as the number of resources used by the resident at the evolutionary branching point the single initial resident is attracted to (e.g., three for the example depicted in Fig. 5C–E). This number can be lower than the maximal dimensionality that can be convergence stable for a given  $\alpha$ , and so the outcome depends on the details of how the basins of attraction for the different evolutionarily singular points are configured globally in trait space.

### 3.2. Example 2: a more elaborate resource-competition model

The above example, due to its relative simplicity, is somewhat limited in the types of outcomes that can arise, with each consumer in an assembled community either being a generalist consuming all resources equally or a full specialist consuming only a single resource. To examine a model where other outcomes are possible, we extend a two-resource model by Wickman et al. (2019) to  $d$  dimensions. The model varies not only the trade-off type (generalist-favoring to specialist-favoring), but also the types of the resources, ranging from substitutable to

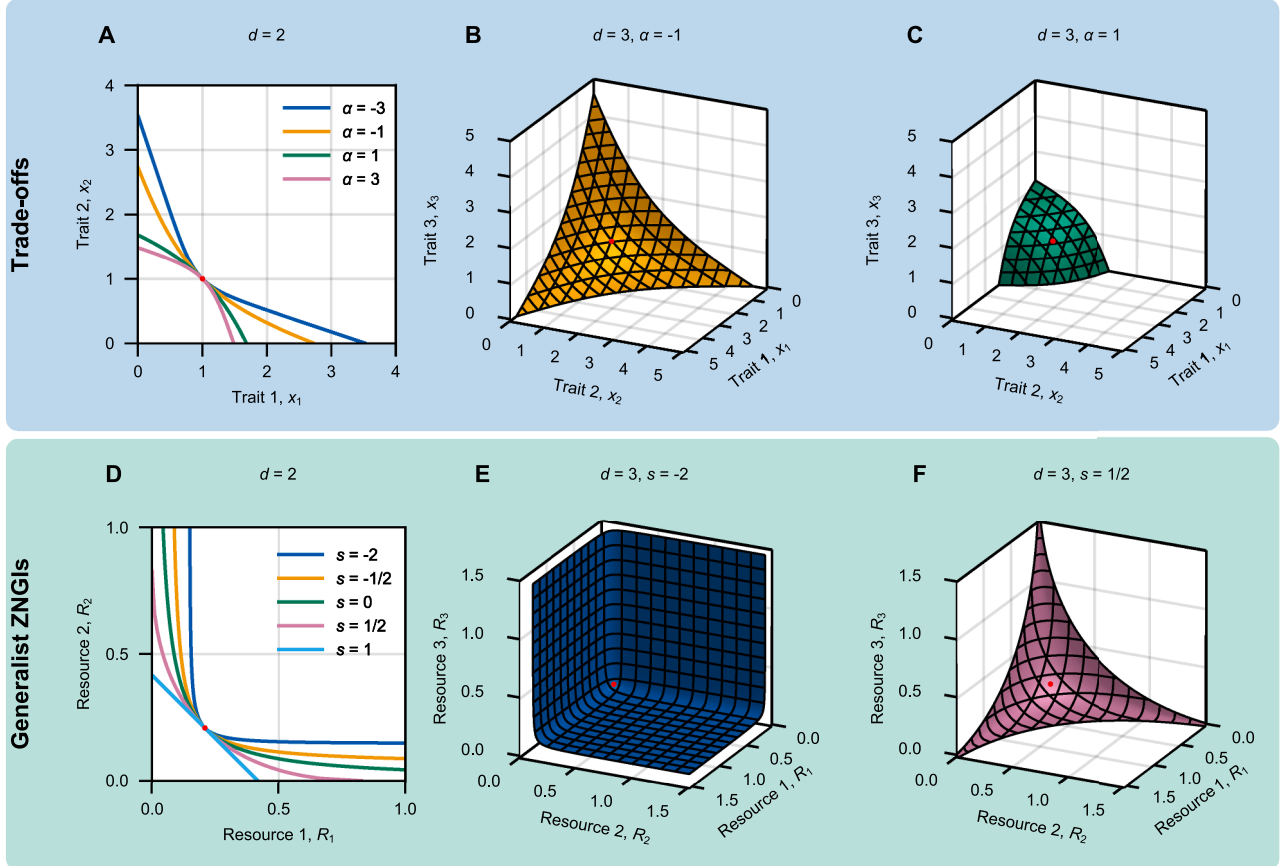


**Fig. 6.** Example trade-offs and ZNGIs for example model 2. (A–C) Examples of trade-offs between resource affinities for dimensionalities  $d = 2$  and  $d = 3$ . Trade-off parameters  $\alpha < 0$  yield specialist-favoring trade-offs and trade-off parameters  $\alpha > 0$  yield generalist-favoring trade-offs. For all values of  $d$  and  $\alpha$ , the trade-off manifold contains the point  $\mathbf{x}^* = (1, 1, \dots, 1)$ , marked with a red dot in each panel. (D–F) Examples of zero net growth isomanifolds (ZNGIs) for generalist consumers with trait components given by  $\mathbf{x}^* = (1, 1, \dots, 1)$ . The ZNGIs denote the resource combinations  $\mathbf{R} = (R_1, R_2, \dots, R_d)$  for which  $g(\mathbf{x}^*, \mathbf{R}) = 0$ . The type of the resources are determined by the substitutability parameter  $s$  so that for  $s = 1$  resources are perfectly substitutable, for  $0 < s < 1$  resources are complimentary substitutable and for  $s < 0$ , resources are interactive essential. For all values of  $d$  and  $s$  the ZNGI contains the point  $\mathbf{R}^* = (R^*, R^*, \dots, R^*)$  where  $R^* = (m^{-1} - G_{\max}^{-1})^{-1}$ , marked with a red dot in each panel.

essential (sensu Tilman 1980). In our previous example, the trade-offs were constructed so that the ‘endpoints’ of the trade-off were fixed with one trait component being equal to one and the rest zero. To accommodate essential resources, Wickman et al. (2019) instead constructed trade-offs in such a way that all trade-offs went through the midpoint  $(x_1, x_2) = (1, 1)$ . Here, we generalize this trade-off to  $d$  dimensions so that  $(x_1, \dots, x_d) = (1, \dots, 1)$  is on the trade-off for all dimensionalities and trade-off types. Specifically, generalizing the trade-off of Wickman et al. (2019) to  $d$  dimensions yields (Supplementary S2.1)

$$h(\mathbf{x}) = \left( \prod_{i=1}^d e^{\alpha(x_i-1)} \right)^{\frac{1}{\beta}} \left( \sum_{i=1}^d e^{\alpha(x_i-1)} - d + 2 \right) - 2 = 0, \quad (30)$$

where  $\alpha < 0$  yields specialist-favoring trade-offs and  $\alpha > 0$  yields generalist-favoring trade-offs (Fig. 6A–C). The parameter  $\beta$  controls how large a single trait can become under full specialization for specialist-favoring trade-offs. The trade-off is constructed in such a way that when fixing any trait component in  $d$  dimensions to be one, the trade-off among the remaining trait components is identical to the trade-off for  $d-1$  dimensions. Thus, for example, fixing  $x_1 = 1$  in Fig. 6B, the trade-off curve between  $x_2$  and  $x_3$  is the one depicted in Fig. 6A with  $\alpha = -1$ .

Generalizing the two-resource per capita growth function of Wickman et al. (2019) to  $d$  resources yields

$$G(\mathbf{x}, \mathbf{R}) = \frac{1}{\frac{1}{G_{\max}} + \frac{1}{T(\mathbf{x}, \mathbf{R})}}, \quad T(\mathbf{x}, \mathbf{R}) = \left( \frac{1}{d} \sum_{i=1}^d (x_i R_i)^s \right)^{\frac{1}{s}}, \quad (31)$$

where  $G$  is an increasing function in all resources, saturating at  $G_{\max}$ . The parameter  $s$  governs the extent to which the resources are mutually substitutable or essential, with resources being perfectly substitutable for  $s = 1$  and completely essential for  $s \rightarrow -\infty$ . Specifically, for  $s = 1$ , the per capita growth function is equivalent to a Holling Type-II function with attack rate  $x_i/d$  for resource  $i$  and equal handling time  $1/G_{\max}$  for all resources, and for  $s \rightarrow -\infty$  the per capita growth function is a saturating version of Liebig’s law of the minimum with  $T(\mathbf{x}, \mathbf{R}) = \min(x_1 R_1, x_2 R_2, \dots, x_d R_d)$ . For  $1 > s > 0$ , resources are complimentary substitutable and for  $0 > s > -\infty$ , resources are interactive-essential (see Tilman 1980; Schreiber and Tobiason 2003; Wickman et al. 2019 for details). The growth function is constructed in such a way that for a consumer with  $\mathbf{x} = (1, 1, \dots, 1)$ , for all values of  $d$  and  $s$ , the zero-net-growth isocline (ZNGI) goes through the same point in resource space, see Fig. 6D–F for examples.

The complete set of equations governing the consumer–resource system for a single consumer with density  $N$  and trait vector  $\mathbf{x}_{\text{res}}$  is

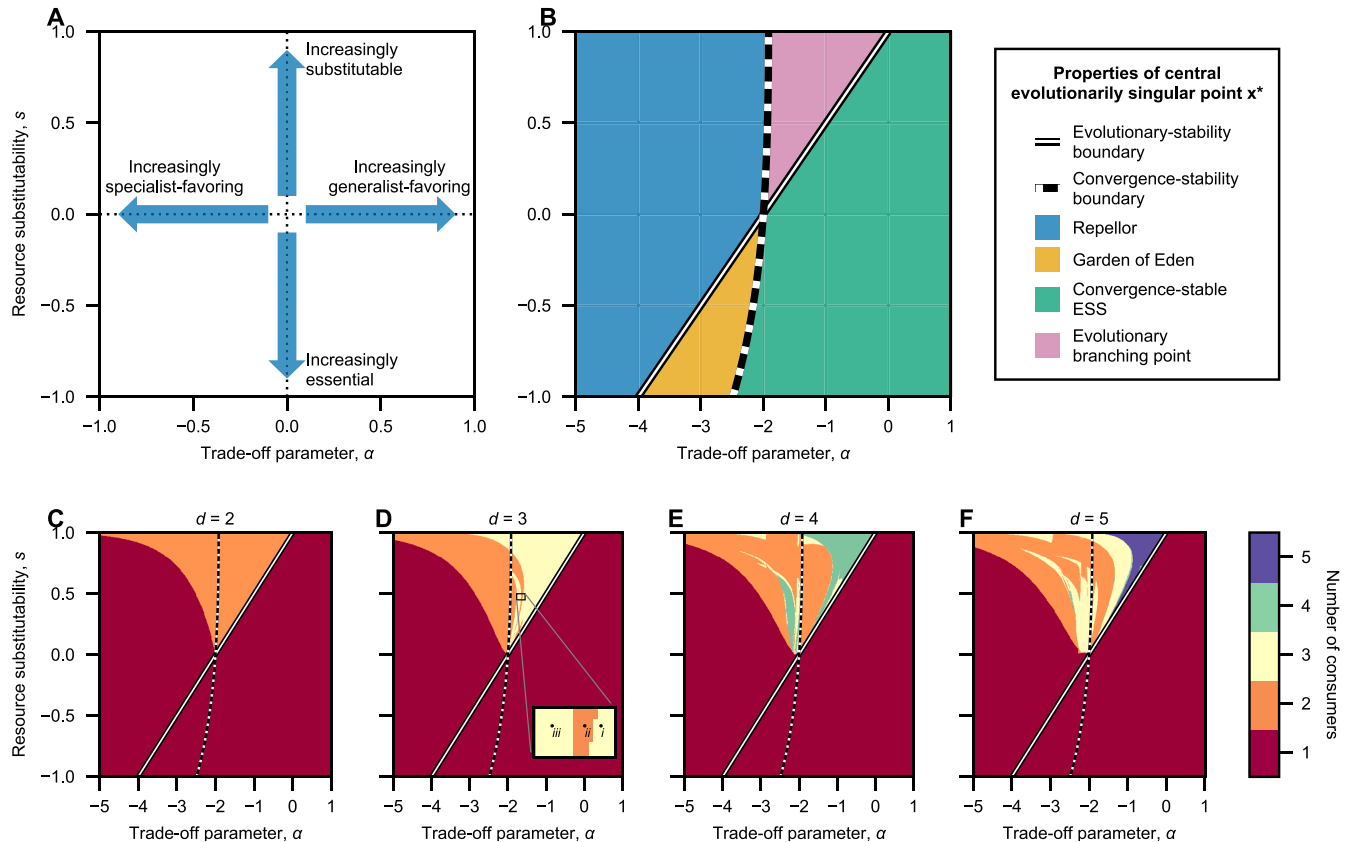


**Fig. 7.** Outcomes for example model 2. (A) Diagram depicting the effects of varying the parameters  $s$  and  $\alpha$ . (B) Characteristics of the central evolutionary singular point  $\mathbf{x}^* = (1, 1, \dots, 1)$ .  $\mathbf{x}^*$  is evolutionarily stable to the right of the white line with black borders, and convergence stable to the right of the white-black dotted line. Numerical solutions (panels C–F) indicate that neither of these boundaries depend on the dimensionality  $d$ . (C–F) Number of consumers assembled through successive evolutionary branching with initial conditions given by a single consumer with a trait close to  $\mathbf{x}^* = (1, 1, \dots, 1)$ . The two black-and-white lines denote the same boundaries as in panel B. Although we computed each set of lines separately for each dimensionality  $d$ , they are, up to numerical error, exactly the same for each  $d$ . The inset in panel D shows the location in parameter space for the three communities depicted in detail in Fig. 9. Other parameter values:  $G_{\max} = 5$ ,  $m = 0.2$ ,  $r = 1$ ,  $K = 5$ ,  $\beta = 2$ .

given by

$$g(\mathbf{x}, \mathbf{R}) = G(\mathbf{x}, \mathbf{R}) - m, \quad (32a)$$

$$\frac{dN}{dt} = g(\mathbf{x}_{\text{res}}, \mathbf{R})N, \quad (32b)$$

$$\frac{dR_i}{dt} = r(K - R_i) - C_i(\mathbf{x}_{\text{res}}, \mathbf{R})G(\mathbf{x}_{\text{res}}, \mathbf{R})N, \quad (32c)$$

$$C_i(\mathbf{x}, \mathbf{R}) = \frac{(x_i R_i)^E}{\sum_{j=1}^d (x_j R_j)^E}, \quad E = \exp(s - 1), \quad (32d)$$

where  $C_i$  is the proportion of total resource uptake that is from resource  $i$ .

For all values of  $s$ ,  $\alpha$ , and  $d$ , the trait vector  $\mathbf{x}^* = (1, 1, \dots, 1)$  is an evolutionarily singular point (Supplementary S2.2). As we did for our simple resource model, we can investigate the properties of this point with respect to evolutionary and convergence stability, and see how the joint effects of trade-off type (governed by  $\alpha$ ) and resource type (governed by  $s$ ) affect how many consumers can be assembled through successive evolutionary branching.

We can calculate that the evolutionarily singular point  $\mathbf{x}^*$  is evolutionarily stable whenever (Supplementary S2.3)

$$\alpha > \left(1 + \frac{2}{\beta}\right)(s - 1). \quad (33)$$

In words, this implies that for less-substitutable resources (smaller  $s$ ), evolutionary stability is more easily attained, and even specialist-favoring trade-offs can yield evolutionary stability provided resources are not too substitutable. As in our first example, evolutionary stability

does not depend on the dimensionality  $d$ . The model is too complicated to work out analytically the criterion for convergence stability, but numerical calculations strongly suggest that while convergence stability of  $\mathbf{x}^*$  does depend on  $s$  and  $\alpha$ , it does not depend on  $d$ . As opposed to our simple resource model in example 1, the stability characteristics of the generalist strategy are thus entirely independent of the dimensionality of the resource and trait spaces in this model, likely due to the fact that we are generalizing the trade-off around a midpoint rather than around the edges. We depict the stability of  $\mathbf{x}^*$  across different trade-off and resource types in Fig. 7B. Evolutionary branching at  $\mathbf{x}^*$  is only possible for substitutable resources ( $s > 0$ ), and the ranges of trade-offs that yield evolutionary branching get increasingly narrow as resources become less substitutable (Fig. 7B).

For our simple resource model in example one, numerical experiments suggested that a fully saturated community with the same number of consumers as resources could be assembled through successive evolutionary branching if and only if the central evolutionarily singular point was a branching point. For our more elaborate model, this implication generally does not hold in either direction. In Fig. 7C–F we depict the final number of consumers assembled through successive evolutionary branching for  $d = 2$  to  $d = 5$  where the initial condition was a single consumer with a trait very close to, but not exactly at, the evolutionarily singular point  $\mathbf{x}^* = (1, 1, \dots, 1)$ .

For  $d = 2$  (Fig. 7C), we see that while  $\mathbf{x}^*$  being a branching point is a sufficient condition for evolving a saturated community, it is not necessary, and a saturated community can evolve even when  $\mathbf{x}^*$  is a repellor. This is because as  $\alpha$  decreases past the point of converge stability the

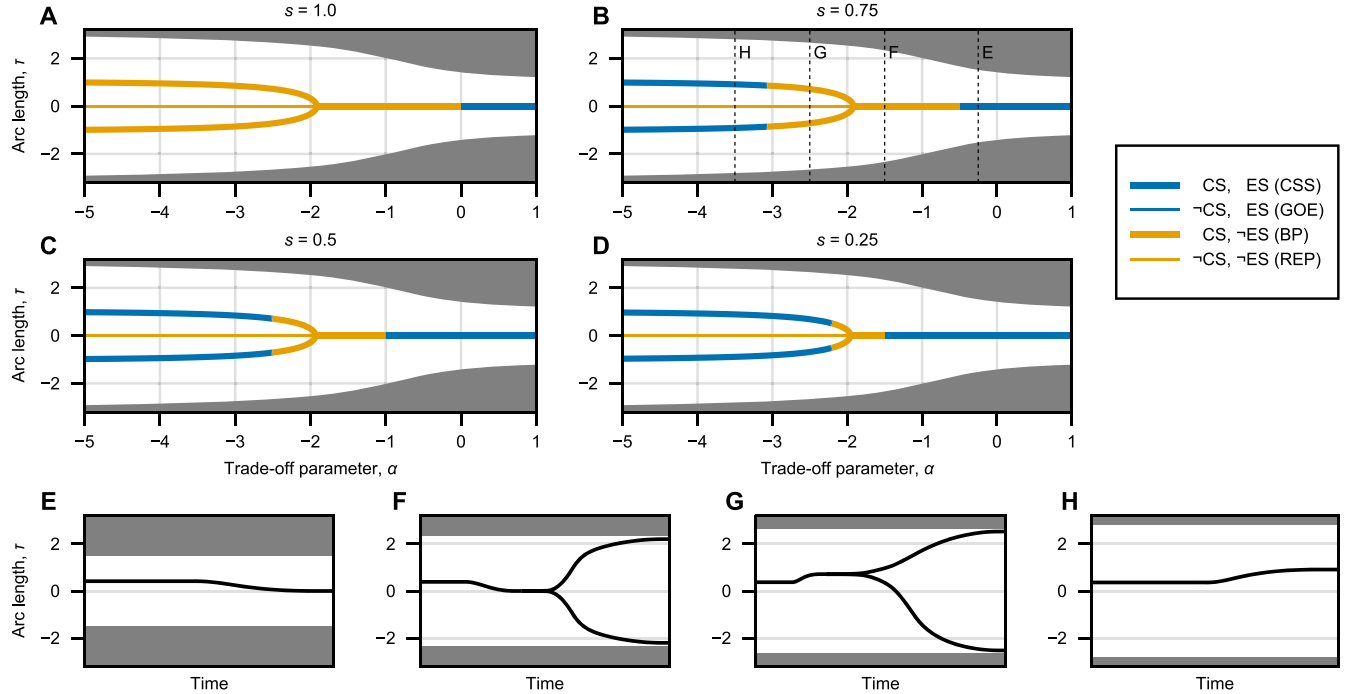


**Fig. 8.** Bifurcation diagrams and example outcomes for example model 2 for  $d = 2$ . (A–D) Each panel shows a horizontal transect of Fig. 7C for a single consumer species. The y-axis in each panel is an arc-length parameterization of the trade-offs depicted in Fig. 6A, re-centered so that  $\tau = 0$  corresponds to  $(x_1, x_2) = (1, 1)$ , with  $\tau < 0$  indicating higher affinity for resource two, and  $\tau > 0$  indicating higher affinity for resource 1. As the trade-off parameter changes, so does the total length of trade-off curves, and the dark gray areas in each panel are outside the boundaries of the trade-off curve. Going from right to left in each panel (increasingly specialist-favoring trade-offs), the central evolutionarily singular point  $\tau = 0$  goes from being a convergence stable ESS, to an evolutionary branching point, to an evolutionary repellor, at which point there is a pitchfork bifurcation and two new evolutionarily singular points that are branching points appear. For  $s < 1$ , these branching points becomes CSSs for sufficiently specialist-favoring trade-offs. Legend CS: Convergence Stable, ES: Evolutionarily stable, CSS: Convergence-stable evolutionarily stable strategy, GOE: Garden of Eden, BP: Branching point, REP: Repellor. (E–H) Example assembly trajectories for the parameter values cross-referenced in panel B.

system undergoes a pitchfork bifurcation with a new branching point appearing on either side of  $x^*$  (Fig. 8). When resources are not perfectly substitutable ( $0 < s < 1$ , Fig. 8B–D), as we make the trade-off increasingly specialist-favoring we first get a single generalist as the outcome (Fig. 8E), then a two-consumer community that branched at the generalist strategy (Fig. 8F), then a two-consumer community that branched at an off-center attractor (Fig. 8G), and finally a single partially specialized consumer (Fig. 8H).

For  $d \geq 3$  (Fig. 7),  $x^*$  being a branching point is neither necessary nor sufficient for attaining a fully saturated community, and the number of consumers in the final community is non-monotonic in  $d$ ,  $\alpha$ , and  $s$ . To get a better sense of how some of the idiosyncratic diversity patterns come about, in Fig. 9 we depict the community-assembly process for the three communities marked in the inset of Fig. 7D. At the point labeled *i* (Figs. 7D, 9A–C), the final community is a community of three consumers where each consumer has a favored resource and two equally non-favored resources (a partial specialist), and at the point labeled *iii* (Figs. 7D, 9F–H), the final community is a community where each consumer has two equally favored resources and one non-favored resource (a partial generalist). In between these two communities in parameter space is the point labeled *ii* (Figs. 7D, 9D–E), where the final community comprises one partial specialist and one partial generalist. For greater values of  $\alpha$  (as in *i*), the partial generalist would have branched into two partial specialists, and for lesser values of  $\alpha$  (as in *iii*), the partial specialist would have branched into partial generalists, but for the small intermediate range of  $\alpha$  values around *ii*, neither is possible.

#### 4. Discussion

In this paper we developed techniques for combining an implicitly defined trade-off with resource-competition and adaptive-dynamics the-

ory to explore how the joint effects of the number of resources and the shape of the trade-off between resource-uptake affinities determined eco-evolutionary outcomes. In two example models of resource competition that have been previously studied for two resources we showcased some of the consequences of increasing the number of resources for which consumers compete.

Eco-evolutionary resource-competition models have to date relied primarily on using parameterizations to describe trade-offs between resource-related traits under selection in competition for two resources (Lawlor and Smith, 1976; Schreiber and Tobiason, 2003; Rueffler et al., 2006; Wickman et al., 2019; Vasconcelos and Rueffler, 2020). Parameterizations for two dimensions are, however, difficult to generalize to competition for more resources involving more traits. Here, similarly to Ito and Sasaki (2016), by formulating the trade-off as an implicit relation we could easily generalize trade-offs to arbitrary dimensionalities. Ito and Sasaki (2016) used a Lagrange-multiplier method to derive their conditions for evolutionary and convergence stability, rather than the projection-function approach we have used here. The conditions of both methods are, of course, equivalent, and which formulation one finds easier to work with will vary from model to model and depend on personal preference. Given our focus here on resource competition, or more generally, interaction mediated through limiting factors (Chase and Leibold, 2003; Koffel et al., 2021), we have additionally derived expressions for how these limiting factors enter into the expressions for the selection Hessian and Jacobian (Eqs. (12), (19)), yielding expressions that are directly evaluable from model ingredients. This has two main benefits. First, even when an ecological model cannot be solved analytically for all resident trait vectors, it may still be possible to solve it for an evolutionarily singular point. When this is the case, our expression for the selection Jacobian can be used to evaluate the convergence stability, as was the case for our first example

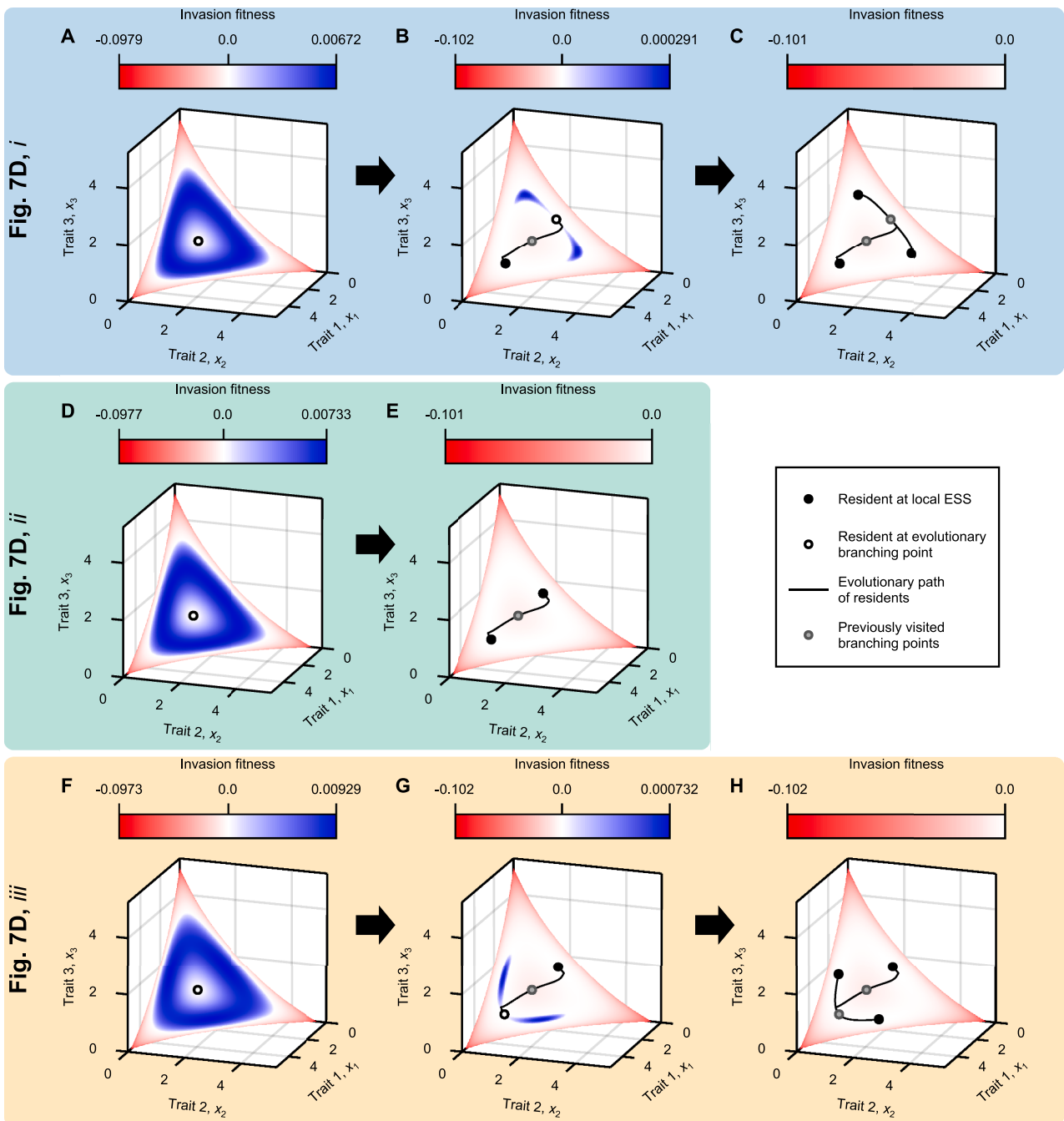


**Fig. 9.** Community assembly for the inset in Fig. 7D. The top row depicts the community assembly for community *i*, the middle row for community *ii*, and the bottom row for community *iii* in the inset in Fig. 7D. Each black dot is resident in the community at an evolutionarily singular point, and the color scale on the trade-off surface depicts in the invasion fitness of rare invaders. The black lines depict the evolutionary paths of residents leading up to each evolutionarily singular point. Note that while the color scales are linear on either side of zero, they differ in magnitude in the positive and negative directions.

model (see Supplementary S1.2 for details). Second, as these expressions depend only on the model ingredients and their derivatives, using modern programming techniques like automatic differentiation (we used the ForwardDiff.jl package in the Julia programming language; Revels et al. 2016), these expressions are easily implementable in a generic way in computer code. The upshot of this is that once this is done, specifying a specific model requires only a few lines of code describing the trade-off, the per capita growth function, and the equations for the limiting factors (see the file `illustrative_example_code.jl` in the supplementary code for an example), which enables quick numer-

ical exploration of different models and trade-offs with minimal code alterations.

While providing great utility in moving between dimensionalities, implicit trade-off formulations have some clear drawbacks compared to parameterization. For one, locating points on the trade-off is more involved than for a typical parameterization, where parameters are usually taken to be inside a rectangular or other simple domain. This also makes computing the global fitness landscape considerably more involved for the implicit formulation. For two and three dimensions there are well-established numerical techniques for finding level sets of

functions, which we used to calculate the fitness landscapes depicted in Figs. 4 and 9, but for higher dimensionalities, computing the global fitness landscape is a challenge. However, beyond a certain dimensionality, this problem is no longer specific to the implicit formulation, as the curse of dimensionality makes computing a fitness landscape in, say, twenty-dimensional space unfeasible also for parameterized trade-offs.

Regardless of how trade-offs are implemented, multivariate adaptive dynamics has subtleties that, for the sake of simplicity, we have for the most part glossed over in this paper. While evolutionary stability is relatively straight-forward also in higher dimensions, convergence stability in higher trait dimensions comes with a suite of complications (Leimar, 2001, 2009; Geritz et al., 2016). For example, an evolutionarily singular point may be convergence stable for some, but not all, mutational variance-covariance matrices (see Vasconcelos and Rueffler, 2020 for an example in a two-resource model). Our analysis of the central evolutionarily singular points in our two example models is, however, simplified by the fact that the symmetry of the models yield symmetric selection Jacobians, and convergence stability is strictly determined by the leading eigenvalue of the Jacobian. Our more elaborate model in Example 2 could well have non-central evolutionarily singular points whose convergence stability may depend on the mutational variance-covariance matrix. This brings us to the broader point of mutational variance-covariance matrices and how to interpret them under our projections. To keep the models simple, and to mimic the symmetry of the rest of the models, for our numerical simulations, we simply let evolution follow in the direction of the projected selection gradient. This could be interpreted as the projection of mutations drawn from a distribution of mutations whose variance-covariance matrix is diagonal with equal (and very small) variances for all trait directions. Another way to view directional selection in our model, explored in detail by Ito and Sasaki (2020), is that the coordinate-dependent projection matrix  $\partial y_k / \partial x_i$  is the mutational variance-covariance matrix, but that this matrix is only positive semidefinite, with an eigenvalue of zero in the direction orthogonal to the trade-off surface at all points.

Whether one uses the projection formalism we have developed here, classic parameterization, or embedding the trade-off into a trait-dependent mutational variance-covariance matrix, there are degrees of freedom in specifying these while still obeying the trade-off. Apart from local-stability considerations, different choices are likely to affect outcomes like the adaptive radiations we studied for our two example models, as different choices can alter the global shape of the basins of attraction for various evolutionarily singular points. In this paper, we chose local orthogonal projection to describe the projection function for its mathematical properties in lieu of any data giving biological guidance on how to choose the projection, and as it allowed us to relatively easily derive expressions for the local projection directly in terms of the trade-off functions (Eqs. (16) and (18)). Still, if one were able to obtain empirical information regarding how the projections should be constructed for a particular system, one could still use Eqs. (12) or (13) to adapt our methodology to this system. On a final note regarding how details of implementation can affect outcomes, if one employs the canonical equation of adaptive dynamics (Dieckmann and Law, 1996; Champagnat, 2003) rather than the simplified form we used here for directional trait evolution (Eq. (29)), the dependence of the canonical equation on the density of the residents for the speed of evolution could also deform the basins of attraction.

To better understand the joint role of trade-off shapes and the number of resources under competition, we applied our derived methods to two models of resource competition. Our first example model is adapted from a family of eco-evolutionary two-resource models (Lawlor and Smith, 1976; Rueffler et al., 2006) and constructed to be as simple as possible. In this family of models, varying the trade-off strength from generalist-favoring to specialist-favoring, the central evolutionarily singular point typically changes from a convergence stable ESS to a branching point to a repeller, and finally to unviability as the trade-off became increasingly specialist-favoring. Our model retains this sequence for all

dimensionalities  $d$  (Fig. 5A), but while the transition from a convergence stable ESS to a branching point always occurs at  $\alpha = 1$ , higher dimensionalities transition to a repeller and unviability for increasingly less specialist-favoring trade-offs. Our model is very similar to the model analyzed by Caetano et al. (2021), with the only real difference being that they used a Monod function for uptake, taking the maximum uptake rates for each resource to be the trait vector for each species. More crucially, and the reason we have nevertheless analyzed the model here, is that using an approximation where the resource supply rate ( $rK$  in our model) was positive but the leaching rate ( $-rR$  in our model) was zero, they found that the central evolutionarily singular point was always convergence stable. This shows that small changes in model assumptions have the potential to qualitatively shift eco-evolutionary outcomes, and that some caution may be required when extrapolating results.

For  $d > 2$  and when the central evolutionarily singular point is not evolutionarily stable, the model is multistable, and the final evolved community depends on initial conditions. This applies not just to which resources end up being exploited, but to the richness of the final community as well. Interestingly, in spite of the simplicity and symmetry of the model, the richness of the final evolved community can depend on initial conditions in a somewhat surprising manner. One might expect that evolved diversity would be maximized when starting near the center of trait space, but, for example, for  $d = 7$  and  $\alpha = 0.4$ , starting the eco-evolutionary assembly process with a single consumer with near-equal affinities for all seven resources yields a final evolved community with two consumers (Fig. 5B), whereas if the initial condition is instead set to be a single consumer with near-equal affinity for four of the resources and near-zero affinity for the remaining three, a community of four consumers evolves. Similarly to the two-resources models, regardless of initial conditions, whenever  $\alpha < 1$ , each consumer in the final community will consume only one of the resources.

To study a case where full specialization or full generalism are not the only two possible outcomes, we extended a two-resource competition model by Wickman et al. (2019) who varied not only the trade-offs, but also the resource types—ranging from substitutable to essential (Tilman, 1980; Schreiber and Tobiason, 2003). For  $d = 2$ , our model is exactly equal to the model of Wickman et al. (2019) (Supplementary S2.1), and thus our results for the stability characteristics of the central evolutionarily singular point are the same (Fig. 7B). For our generalization to  $d$  resources and traits, the stability characteristics of the central evolutionarily singular point does not change with dimensionality for given trade-offs and resource types (Fig. 7C–F), although the absolute magnitude of the eigenvalue describing evolutionary stability decreases with increasing dimensionality (Supplementary S2.3). Another outcome of the two-resource model that remains unchanged with increasing dimensionality is the lack of diversity that can evolve for essential resources ( $s < 0$ ). For two resources, the model is set up in such a way that when resources are essential, at the equilibrium point the consumption vectors are such that the two consumers do not consume relatively more of the resource that limits them more, making coexistence unstable (Wickman et al., 2019). Scaling up to multiple resources does not alter this general pattern where a single consumer consumes resources it is not primarily limited by, preventing coexistence. What does substantially change when the dimensionality is increased are the patterns of richness that can evolve for different resource types ( $s$ ) and trade-off types ( $\alpha$ ). Like our first simple example model, the evolved richness is not necessarily increasing in the dimensionality for any given  $s$  and  $\alpha$ . For example, with  $s = 0.5$  and  $\alpha = -1.5$ , for  $d = 3$ , three coexisting consumers evolve whereas for  $d = 4$ , only two consumers emerge. Unlike our simpler model, evolved richness can also be highly non-monotonic in the trade-off strength  $\alpha$  for given values  $d$  and  $s$ , and equally diverse communities can be qualitatively different (Fig. 7D, inset; Fig. 9). This demonstrates that even for highly symmetric models, the diversity that can emerge through adaptive radiations in multi-resource competition can be highly unpredictable. One predictable aspect both our example models share is that high diversity tends to evolve when trade-offs

are just specialist-favoring enough (just to the left of the evolutionary-stability boundary in Fig. 7). This is close to the point of neutrality for perfectly substitutable resources where an arbitrary number of consumers could coexist neutrally. However, this high diversity is also the least structurally stable, as relatively small changes to the trade-off could cause collapse into monomorphism.

Although we are not aware of any work that jointly varied the number of resources and trade-off types other than Caetano et al. (2021) for a direct comparison, the related question of how trait complexity in competition affects the possibility of diversification through evolutionary branching has seen substantial study. In Lotka–Volterra competition models, increasing the dimensionality of the trait space through which competitors interact has been shown to increase the likelihood of evolutionary branching (Doebeli and Ispolatov, 2010; Débarre et al., 2014; Svardal et al., 2014). In particular, Svardal et al. (2014) showed that this is true when the Lotka–Volterra model is more directly derived from a resource-competition model in the style of MacArthur (1970). These models differ from ours in that rather than increasing the number of distinct resources, what is increased as the trait-space dimensionality goes up is the number of characteristics of the resource, so that the resource is described as a distribution over, for example, the total mass and maximal linear length of seeds. This effectively makes the resources in these models ordered along some axes, which is not the case for our models. This in turn gives rise to several qualitative differences in behavior between these models and ours when the trait-space dimensionality is increased. In the Lotka–Volterra models, convergence stability of the central evolutionarily singular point is independent of dimensionality, but increasing the dimensionality makes the singular point more likely to lose evolutionary stability and become a branching point. In contrast, for our two example models here, evolutionary stability is independent of the dimensionality of the trait space, but for our simple resource model, increasing the dimensionality will generally lead to a loss of convergence stability of the central evolutionarily singular point (Fig. 5A), and for our complex resource model, both evolutionary stability and convergence stability of the central point are unaffected by dimensionality (Fig. 7C–F). This loss of convergence stability was also observed in an explicit two-resource model when the number of traits under selection increased (Vasconcelos and Rueffler, 2020). One pattern that emerges in whether the generalist strategy can lose convergence stability under specialist-favoring trade-offs is that trade-offs among these models that can induce a loss of generalist viability (our Example 1, Vasconcelos and Rueffler 2020) also exhibit a loss of convergence stability whereas models where generalist viability is not affected by the trade-off do not (our Example 2, Doebeli and Ispolatov 2010; Débarre et al., 2014; Svardal et al. 2014; Caetano et al. 2021).

In models in the vein of MacArthur resource competition, adaptive radiations can yield high levels of diversity even when the dimensionality of the trait space is low (Vukics et al., 2003; Ackermann and Doebeli, 2004), whereas in our models the maximum diversity is bounded above by the number of resources. In terms of the total diversity attained via radiation, the total parameter space with regards to the trade-off shape  $\alpha$  and resource substitutability  $s$  that yields a community of at least two consumers does however increase slightly as the dimensionality of the trait space increases for the elaborate resource model (Fig. 7C–F). On the other hand, in terms of reaching a saturated community where the number of consumers equals the number of resources, both our example models suggests that this becomes increasingly difficult as the dimensionality of the trait space increases in the sense that the set of trade-offs that permit saturation shrinks (Figs. 5A and 7C–F). This suggests that even if many distinct resources exist in an environment, it may be unlikely for a single colonizing species to fill niche space through an adaptive radiation with small mutations.

For a single parametric trait, how trade-off shapes qualitatively affect eco-evolutionary outcomes is well studied, and techniques for picking trade-offs in a way that yields a desired outcome, say, an evolutionary branching, exist (de Mazancourt and Dieckmann, 2004; Kisdi,

2015), and there is thus a degree of arbitrariness in how trade-offs are formulated for most models. For our case, the situation is further complicated by the fact that an entire family of trade-offs—one for each dimensionality—needs to be chosen. For our two example models, we chose our trade-off families in such a way as to generalize some of the choices for the original two-resource models we based our examples on. For our simple resource model, the trade-offs in the studies we based this model on (e.g., Lawlor and Smith 1976; Rueffler et al. 2006) were constructed in such a way that the endpoints were the same for all shapes of the trade-off (as in Fig. 1A). We thus generalized these trade-offs to dimensionality  $d$  by ensuring that setting any one trait coordinate to zero would yield the trade-off for dimensionality  $d - 1$ , and that the endpoints (where all but one trait coordinate is zero) were fixed when varying the shape of the trade-off within a dimensionality. Conversely, the model on which we based our elaborate resource model (Wickman et al., 2019) varied the trade-off shape in their two-resource competition model around a fixed midpoint, and here we correspondingly generalized our trade-off to more dimensions around this midpoint. These choices are likely responsible for one of the differences between our two example models, where the convergence stability of the central evolutionarily singular point decreases with increased dimensionality for the simple resource model, but remains unchanged for the complex resource model. Although motivated by the original two-dimensional trade-offs, other choices for how to scale up these trade-offs to arbitrary dimensionalities could have been made, which could qualitatively alter how increased dimensionalities affect outcomes. Ideally, the shapes of multivariate trade-offs and lower-dimensional slices through them would be informed by empirical measurements, but although there is evidence of trade-offs in resource-related traits (Edwards et al., 2011), and the qualitative type of the trade-off (specialist- vs. generalist-favoring) has been determined for pairs of resource types (Schlüter, 1993; Konuma et al., 2013), trade-off data is scarce even for two resources, and we are not aware of any data set suitable for inferring trade-off shapes for multiple resources.

To ensure tractability and to showcase the use of our techniques, we kept certain facets of our example models simple, with high degrees of symmetry. Yet, even our first example, which is about as simple as is conceivable, showed a nontrivial interaction between the number of resources and the shape parameter of the trade-offs (Fig. 5). In spite of its many symmetries, our more complex model showcased rich behavior in terms of the number of evolved coexisting consumers for different trade-off and resource types (Fig. 7). An intriguing aspect of multi-resource competition we have left unexplored in this study is that once more than two resources are in play, trade-offs between subsets of resources need not have the same character, and both generalist- and specialist-favoring trade-off curvatures may operate simultaneously. Similarly, different subsets of resources may be mutually substitutable or essential for the same consumer. Exploring how these combine would be a natural next step in deepening our understanding of the eco-evolutionary dynamics of multi-resource competition.

## Data statement

No data was collected for this study. A zip file with the code used to produce the figures of the manuscript is available through Zenodo doi:10.5281/zenodo.14907850 (Wickman and Klausmeier, 2025).

## Declaration of competing interest

The authors declare the following financial interests/personal relationships which may be considered as potential competing interests: Jonas Wickman reports financial support was provided by National Science Foundation. Christopher A. Klausmeier reports financial support was provided by National Science Foundation. If there are other authors, they declare that they have no known competing financial interests or

personal relationships that could have appeared to influence the work reported in this paper.

## CRediT authorship contribution statement

**Jonas Wickman:** Writing – review & editing, Writing – original draft, Visualization, Software, Methodology, Formal analysis, Conceptualization; **Christopher A. Klausmeier:** Writing – review & editing, Supervision, Funding acquisition, Conceptualization

## Acknowledgments

We thank two anonymous reviewers for comments that helped us improve the manuscript. This work was supported by National Science Foundation grant EF-2124800. This is W. K. Kellogg Biological Station contribution 2412.

## Supplementary material

Supplementary material associated with this article can be found in the online version at [10.1016/j.jtbi.2025.112085](https://doi.org/10.1016/j.jtbi.2025.112085).

## References

- Ackermann M., Doebeli M., 2004. Evolution of niche width and adaptive diversification. *Evolution* 58, 2599–2612. <https://doi.org/10.1111/j.0014-3820.2004.tb01614.x>
- Ashby B., Watkins E., Lourenço J., Gupta S., Foster K.R., 2017. Competing species leave many potential niches unfulfilled. *Nat. Ecol. Evol.* 1, 1495–1501. <https://doi.org/10.1038/s41559-017-0295-3>
- Bowers R.G., Hoyle A., White A., Boots M., 2005. The geometric theory of adaptive evolution: trade-off and invasion plots. *J. Theor. Biol.* 233, 363–377. <https://doi.org/10.1016/j.jtbi.2004.10.017>
- Caetano R., Ispolatov Y., Doebeli M., 2021. Evolution of diversity in metabolic strategies. *eLife* 10, e67764. <https://doi.org/10.7554/eLife.67764>
- Champagnat N., 2003. Convergence of adaptive dynamics n-morphic jump processes to the canonical equation and degenerate diffusion approximation. *Prépubl. Univ. Nanterre (Paris X)* 3.
- Chase J.M., Leibold M.A., 2003. Ecological Niches. University of Chicago Press, Chicago, IL.
- Cressman R., Tao Y., 2014. The replicator equation and other game dynamics. *Proc. Natl. Acad. Sci.* 111, 10810–10817. <https://doi.org/10.1073/pnas.1400823111>
- Débarre F., Nuismer S.L., Doebeli M., 2014. Multidimensional (co)evolutionary stability. *Am. Nat.* 184, 158–171. <https://doi.org/10.1086/677137>
- Dieckmann F., Rinaldi S., 2008. Analysis of evolutionary processes: the adaptive dynamics approach and its applications. Princeton Series in Theoretical and Computational Biology, Princeton University Press, Princeton, NJ.
- DeSantis L.R.G., Pardi M.I., Du A., Greshko M.A., Yann L.T., Hulbert R.C., Louys J., 2022. Global long-term stability of individual dietary specialization in herbivorous mammals. *Proc. R. Soc. B* 289, 20211839. <https://doi.org/10.1098/rspb.2021.1839>
- Dieckmann U., Doebeli M., 1999. On the origin of species by sympatric speciation. *Nature* 400, 354–357. <https://doi.org/10.1038/22521>
- Dieckmann U., Law R., 1996. The dynamical theory of coevolution: a derivation from stochastic ecological processes. *J. Math. Biol.* 34, 579–612. <https://doi.org/10.1007/bf02409751>
- Doebeli M., Ispolatov I., 2010. Complexity and diversity. *Science* 328, 494–497. <https://doi.org/10.1126/science.1187468>
- Edwards K.F., Klausmeier C.A., Litchman E., 2011. Evidence for a three-way trade-off between nitrogen and phosphorus competitive abilities and cell size in phytoplankton. *Ecology* 92, 2085–2095. <https://doi.org/10.1890/11-0395.1>
- Geritz S.A.H., Kisdi E., Meszéna G., Metz J.A.J., 1998. Evolutionarily singular strategies and the adaptive growth and branching of the evolutionary tree. *Evol. Ecol.* 12, 35–57. <https://doi.org/10.1023/a:1006554906681>
- Geritz S.A.H., Metz J.A.J., Rueffler C., 2016. Mutual invadability near evolutionarily singular strategies for multivariate traits, with special reference to the strongly convergence stable case. *J. Math. Biol.* 72, 1081–1099. <https://doi.org/10.1007/s00285-015-0944-6>
- Gonzalez L.M., Proulx S.R., Moeller H.V., 2022. Modeling the metabolic evolution of mixotrophic phytoplankton in response to rising ocean surface temperatures. *BMC Ecol. Evol.* 22, 136. <https://doi.org/10.1186/s12862-022-02092-9>
- Ito H., Sasaki A., 2016. Evolutionary branching under multi-dimensional evolutionary constraints. *J. Theor. Biol.* 407, 409–428. <https://doi.org/10.1016/j.jtbi.2016.07.011>
- Ito H.C., Sasaki A., 2020. Evolutionary branching in distorted trait spaces. *J. Theor. Biol.* 489, 110152. <https://doi.org/10.1016/j.jtbi.2020.110152>
- Kinkel L.L., Bakker M.G., Schlatter D.C., 2011. A coevolutionary framework for managing disease-suppressive soils. *Annu. Rev. Phytopathol.* 49, 47–67. <https://doi.org/10.1146/annurev-phyto-072910-095232>
- Kisdi E., 2015. Construction of multiple trade-offs to obtain arbitrary singularities of adaptive dynamics. *J. Math. Biol.* 70, 1093–1117. <https://doi.org/10.1007/s00285-014-0788-5>
- Koffel T., Daufresne T., Klausmeier C.A., 2021. From competition to facilitation and mutualism: a general theory of the niche. *Ecol. Monogr.* 91, e01458. <https://doi.org/10.1002/ecm.1458>
- Koffel T., Daufresne T., Massol F., Klausmeier C.A., 2016. Geometrical approaches: extending graphical contemporary niche theory to communities and eco-evolutionary dynamics. *J. Theor. Biol.* 407, 271–289. <https://doi.org/10.1016/j.jtpb.2007.12.002>
- Konuma J., Sota T., Chiba S., 2013. A maladaptive intermediate form: a strong trade-off revealed by hybrids between two forms of a snail-feeding beetle. *Ecology* 94, 2638–2644. <https://doi.org/10.1890/12-2041.1>
- Lande R., 1979. Quantitative genetic analysis of multivariate evolution, applied to brain: body size allometry. *Evolution* 33, 402–416. <https://doi.org/10.1111/j.1558-5646.1979.tb04694.x>
- Lande R., 1982. A quantitative genetic theory of life history evolution. *Ecology* 63, 607–615. <https://doi.org/10.2307/1936778>
- Lawlor L.R., Smith J.M., 1976. The coevolution and stability of competing species. *Am. Nat.* 110, 79–99. <https://doi.org/10.1086/283049>
- Leimar O., 2001. Evolutionary change and darwinian demons. *Selection* 2, 65–72. <https://doi.org/10.1556/select.2.2001.1-2.5>
- Leimar O., 2009. Multidimensional convergence stability. *Evol. Ecol. Res.* 11, 191–208.
- Levins R., 1962. Theory of fitness in a heterogeneous environment. I. The fitness set and adaptive function. *Am. Nat.* 96, 361–373. <https://doi.org/10.1086/282245>
- MacArthur R., 1970. Species packing and competitive equilibrium for many species. *Theor. Popul. Biol.* 1, 1–11. [https://doi.org/10.1016/0040-5809\(70\)90039-0](https://doi.org/10.1016/0040-5809(70)90039-0)
- MacArthur R., Levins R., 1967. The limiting similarity, convergence, and divergence of coexisting species. *Am. Nat.* 101, 377–385. <https://doi.org/10.1086/282505>
- de Mazancourt C., Dieckmann U., 2004. Trade-off geometries and frequency-dependent selection. *Am. Nat.* 164, 765–778. <https://doi.org/10.1086/424762>
- Metz J.A.J., Nisbet R.M., Geritz S.A.H., 1992. How should we define ‘fitness’ for general ecological scenarios? *Trends Ecol. Evol.* 7, 198–202. [https://doi.org/10.1016/0169-5347\(92\)90073-k](https://doi.org/10.1016/0169-5347(92)90073-k)
- Middleton D., Svensson H., Scharlemann J.P.W., Faurby S., Sandom C., 2021. Carnnidet 1.0: a database of terrestrial carnivorous mammal diets. *Glob. Ecol. Biogeogr.* 30, 1175–1182. <https://doi.org/10.1111/geb.13296>
- Revels J., Lubin M., Papamarkou T., 2016. Forward-mode automatic differentiation in julia. *arXiv:1607.07892 [cs.MS]* <https://doi.org/10.48550/arXiv.1607.07892>
- Rosenzweig M.L., MacArthur R.H., 1963. Graphical representation and stability conditions of predator-prey interactions. *Am. Nat.* 97, 209–223. <https://doi.org/10.1086/282272>
- Rueffler C., Van Dooren T.J.M., Metz J.A.J., 2006. The evolution of resource specialization through frequency-dependent and frequency-independent mechanisms. *Am. Nat.* 167, 81–93. <https://doi.org/10.1086/498275>
- Sandrinini G., Matthijs H.C.P., Verspagen J.M.H., Muyzer G., Huisman J., 2013. Genetic diversity of inorganic carbon uptake systems causes variation in CO<sub>2</sub> response of the cyanobacterium *microcystis*. *ISME J.* 8, 589–600. <https://doi.org/10.1038/ismej.2013.179>
- Schlüter D., 1993. Adaptive radiation in sticklebacks: size, shape, and habitat use efficiency. *Ecology* 74, 699–709. <https://doi.org/10.2307/1940797>
- Schreiber S.J., Tobaison G.A., 2003. The evolution of resource use. *J. Math. Biol.* 47, 56–78. <https://doi.org/10.1007/s00285-003-0195-9>
- Sheftel H., Szekely P., Mayo A., Sella G., Alon U., 2018. Evolutionary trade-offs and the structure of polymorphisms. *Philos. Trans. R. Soc. B* 373, 20170105. <https://doi.org/10.1098/rstb.2017.0105>
- Siljestam M., Rueffler C., 2024. Heterozygote advantage can explain the extraordinary diversity of immune genes. *eLife* 13, e94587. <https://doi.org/10.7554/eLife.94587>
- Svardal H., Rueffler C., Doebeli M., 2014. Organismal complexity and the potential for evolutionary diversification. *Evolution* 68, 3248–3259. <https://doi.org/10.1111/evo.12492>
- Tilman D., 1980. Resources: a graphical-mechanistic approach to competition and predation. *Am. Nat.* 116, 362–393. <https://doi.org/10.1086/283633>
- Vasconcelos P., Rueffler C., 2020. How does joint evolution of consumer traits affect resource specialization? *Am. Nat.* 195, 331–348. <https://doi.org/10.1086/706813>
- Vukics A., Asbóth J., Meszéna G., 2003. Speciation in multidimensional evolutionary space. *Phys. Rev. E* 68, 041903. <https://doi.org/10.1103/PhysRevE.68.041903>
- Wickman J., Diehl S., Bränström Å., 2019. Evolution of resource specialisation in competitive metacommunities. *Ecol. Lett.* 22, 1746–1756. <https://doi.org/10.1111/ele.13338>
- Wickman J., Klausmeier C.A., 2025. Code for producing the figures for: the effects of trade-off shape and dimensionality on eco-evolutionary dynamics in resource competition. <https://doi.org/10.5281/zenodo.14907850>